^{48}Ca Radius EXperiment – CREX
^{208}Pb Radius EXperiment – PREX

Characterizing the nuclear models informed by PREX and CREX

Tianqi Zhao 趙天奇

Collaborators: Zidu Lin, Bharat Kumar, Andrew Steiner, Madappa Prakash

HHIQCD at YITP, Oct 17, 2024

- arXiv.2406.05267

Network for Neutrinos, Nuclear Astrophysics, and Symmetries
PHYSICS FRONTIER CENTER

OUTLINE

- Nuclear models
- Symmetry energy & Neutron skin experiments (PREX & CREX)
- Tensions between PREX+CREX and mean field models
- Constraints on bulk properties (symmetry energy)
- Constraints on surface properties (spin-orbit coupling)
- Takeaways

Chiral Effective Field Theory (χEFT)

- Low-energy-constant uncertainty: nucleon contact vortex is fitted to light-bound states, e.g. Deuteron.
  Piarulli and Tews 2021
- Regulator uncertainty for EFT: Cut-off $\Lambda = 450\ \text{MeV},\ 500\ \text{MeV}$ tested.
  Entem and Machleidt 2003
- Manybody uncertainty: tested to be subdominant, controlled by model mixing.
  Hu et al. 2022
- Truncation uncertainty for χEFT: modeled with Gaussian Process.
  Drischler et al.

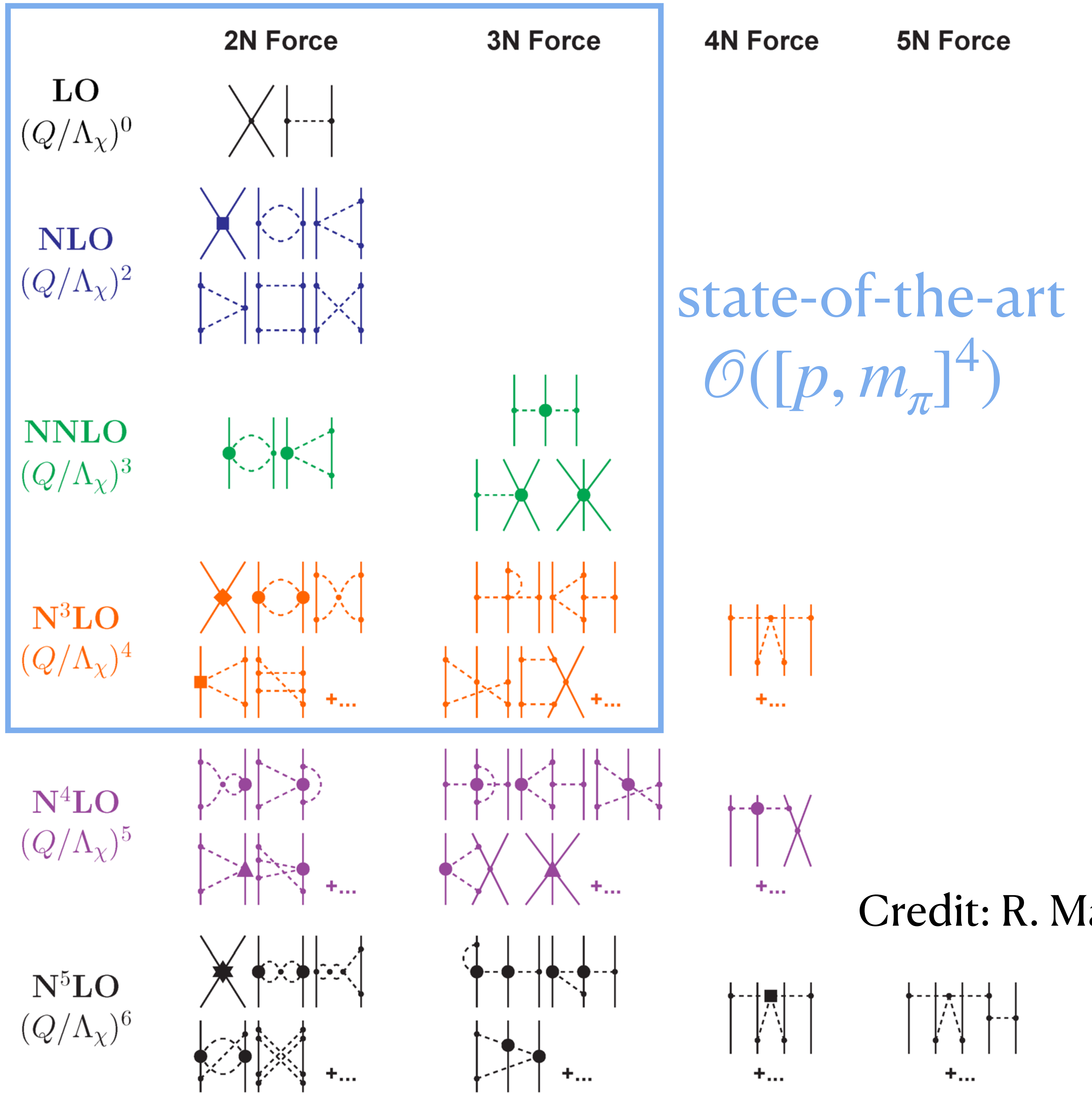

Credit: R. Machleid

Hartree-Fork Approximation

- Nucleon Green's function:
  $G_j(x, x') = < \psi_j(x)\psi_j^\dagger(x') >$

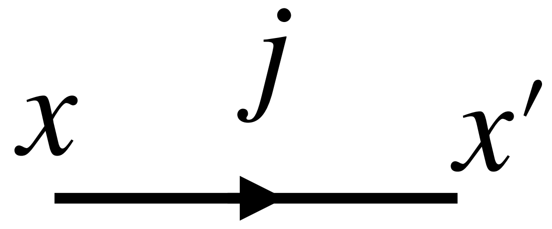

- Two body interactions:
  $V(x, x')$

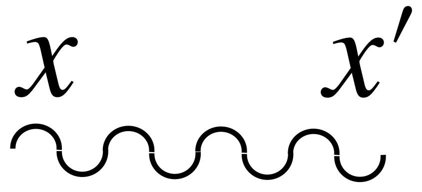

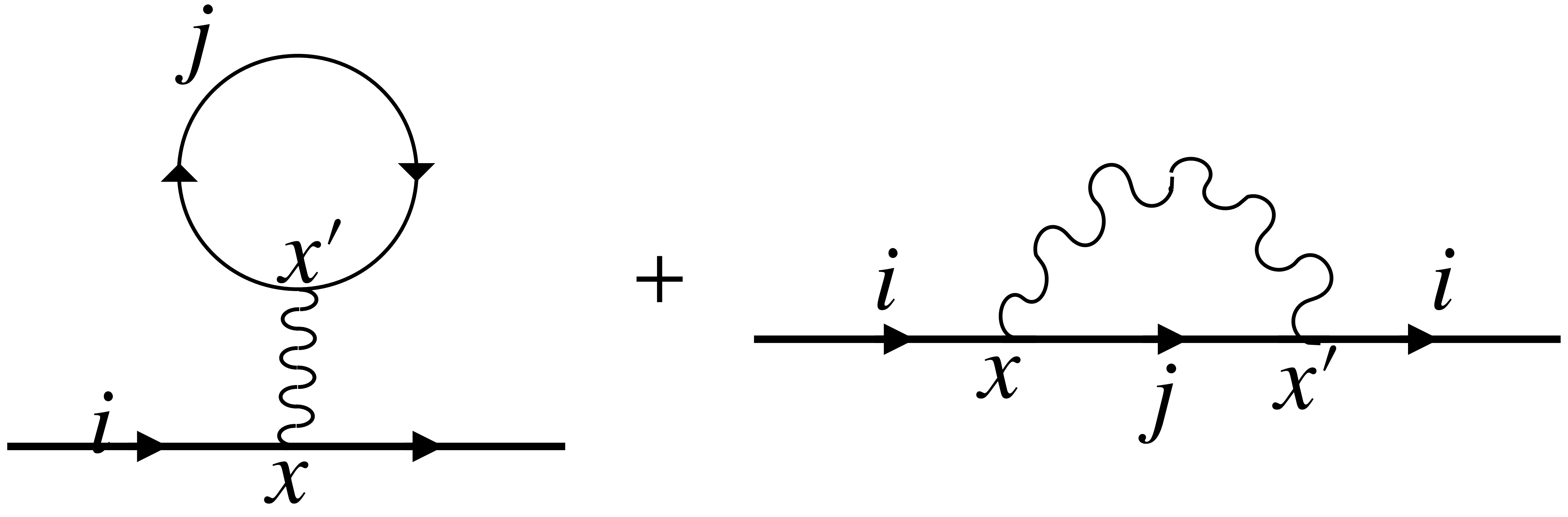

- Hartree potential:
  $$V_{Hartree}(x) = -\sum_j \int V(x, x')G_j(x', x')dx'$$

- Fork potential:
  $$V_{Fock}(x)\psi_i(x) = \sum_j \int V(x, x')G_j(x, x')\psi_i(x')dx'$$

- Schrödinger equation:
  $(H_{kinetic} + V_{Hartree} + V_{Fork})\psi_i = \epsilon_i\psi_i$

- Skyrme model:
  $V(x, x') \propto \delta(r - r') \times$ (spin, momentum)

Relativistic mean-field model (RMF)

Relativistic Hartree Approximation

- 1. Nucleon interactions: e.g. vector isoscalar $g_\omega \psi^\dagger \gamma_\mu \omega^\mu \psi$
  Yukawa interactions mediated by scalar(vector)-isoscalar(isovector) mesons
- 2. Relativistic Hartree potential $V_{Hartree}(x)$:
  from classical meson fields $\sigma(500), \delta(980), \omega(783), \rho(776)$
- 3. Klein–Gordon equation: e. g. $(\square + m^2 + V_{self})\omega = n_p + n_n$
  nucleons source meson fields
- 4. Dirac equation: $(i\gamma^\mu \partial_\mu - m + V_{Hartree})\psi = 0$
  eigenvalue problem determines nucleon levels.
  spin is included automatically in the spinor.

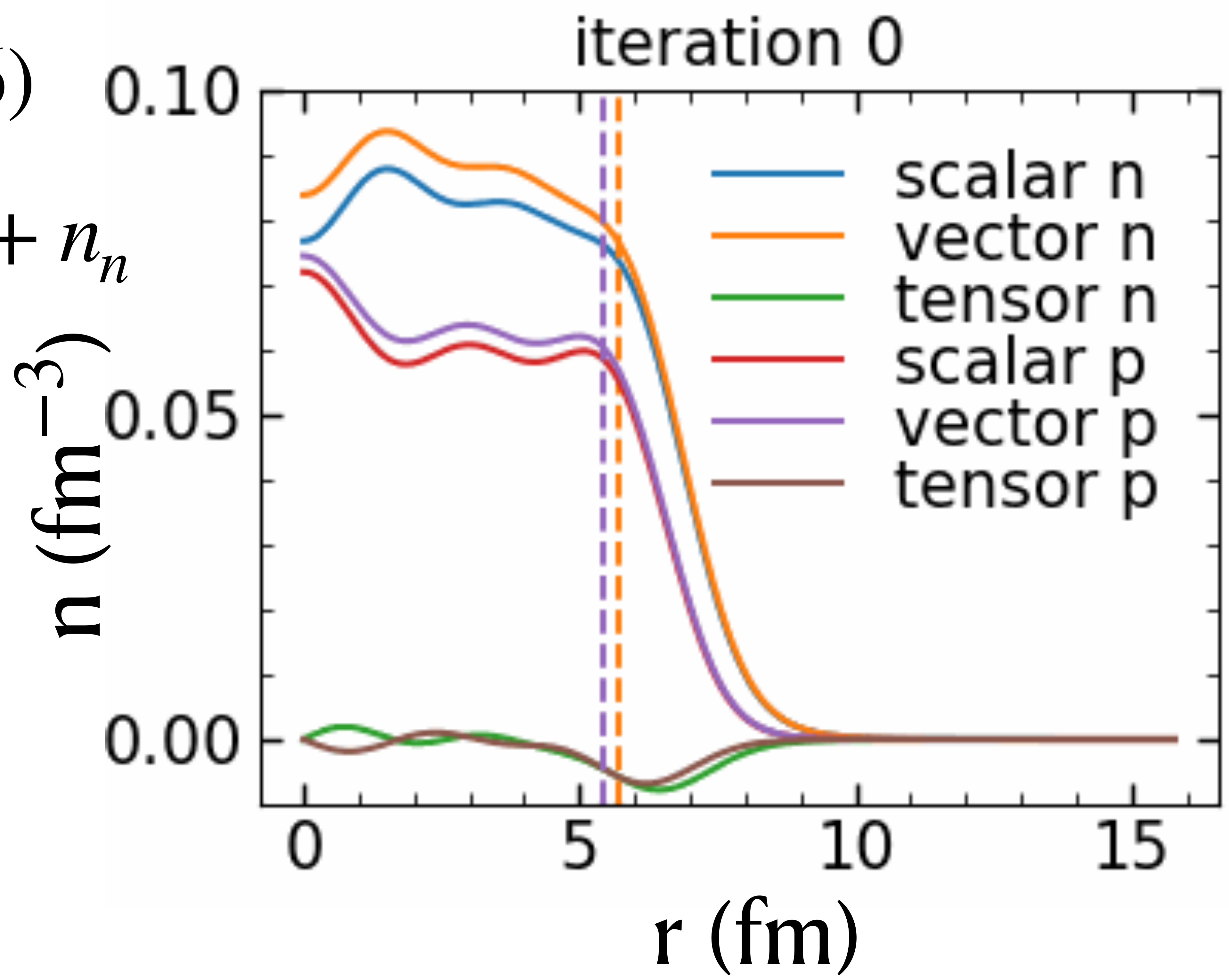

OUTLINE

- Nuclear models
- Symmetry energy & Neutron skin experiments (PREX & CREX)
- Tensions between PREX+CREX and mean field models
- Constraints on bulk properties (symmetry energy)
- Constraints on surface properties (spin-orbit coupling)
- Takeaways

Infinite Nuclear Matter $E(u = n_B/n_s, x = n_p/n_B)$

Neutron star matter ≈ Pure neutron matter = Symmetric nuclear matter + Symmetry energy

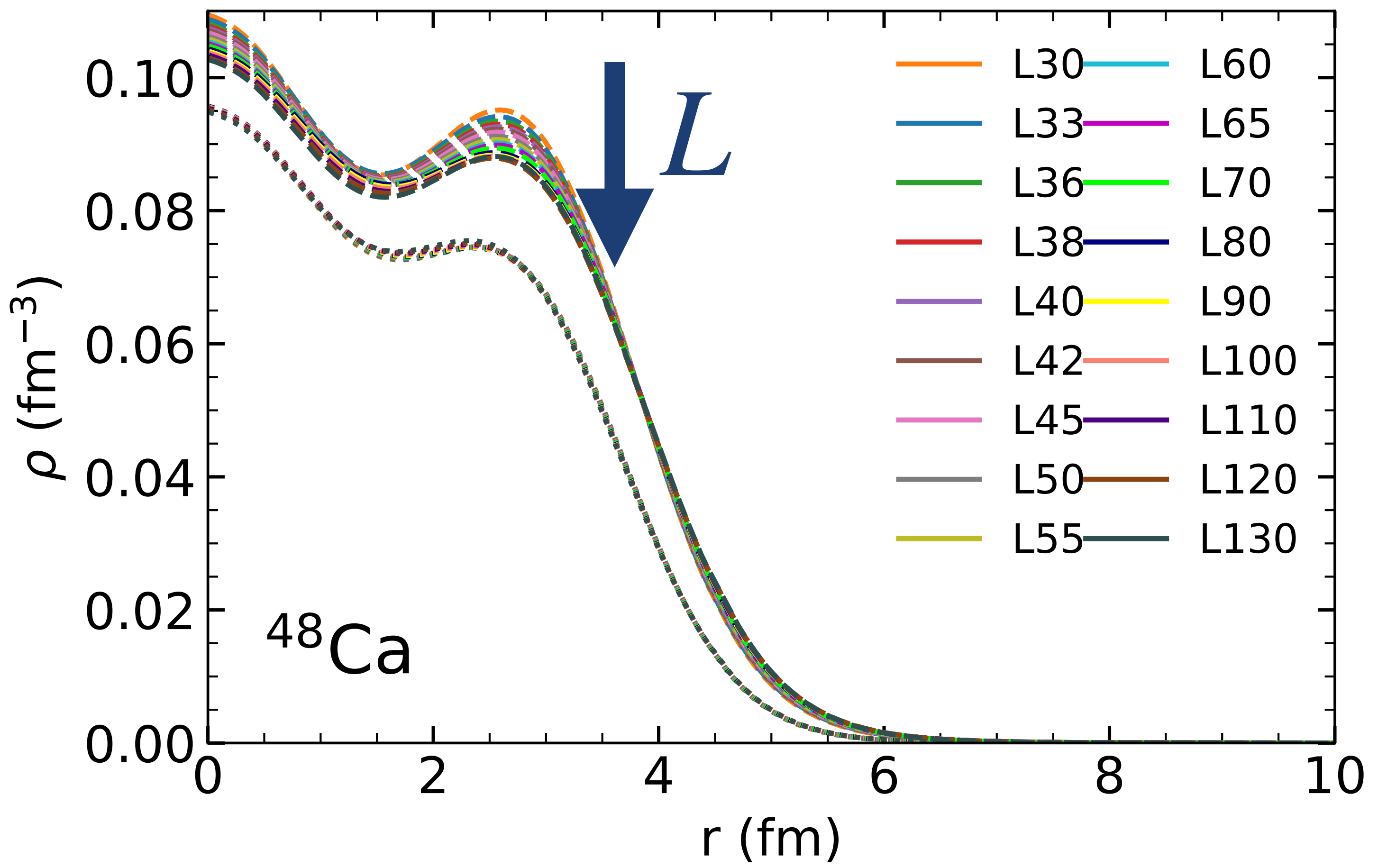

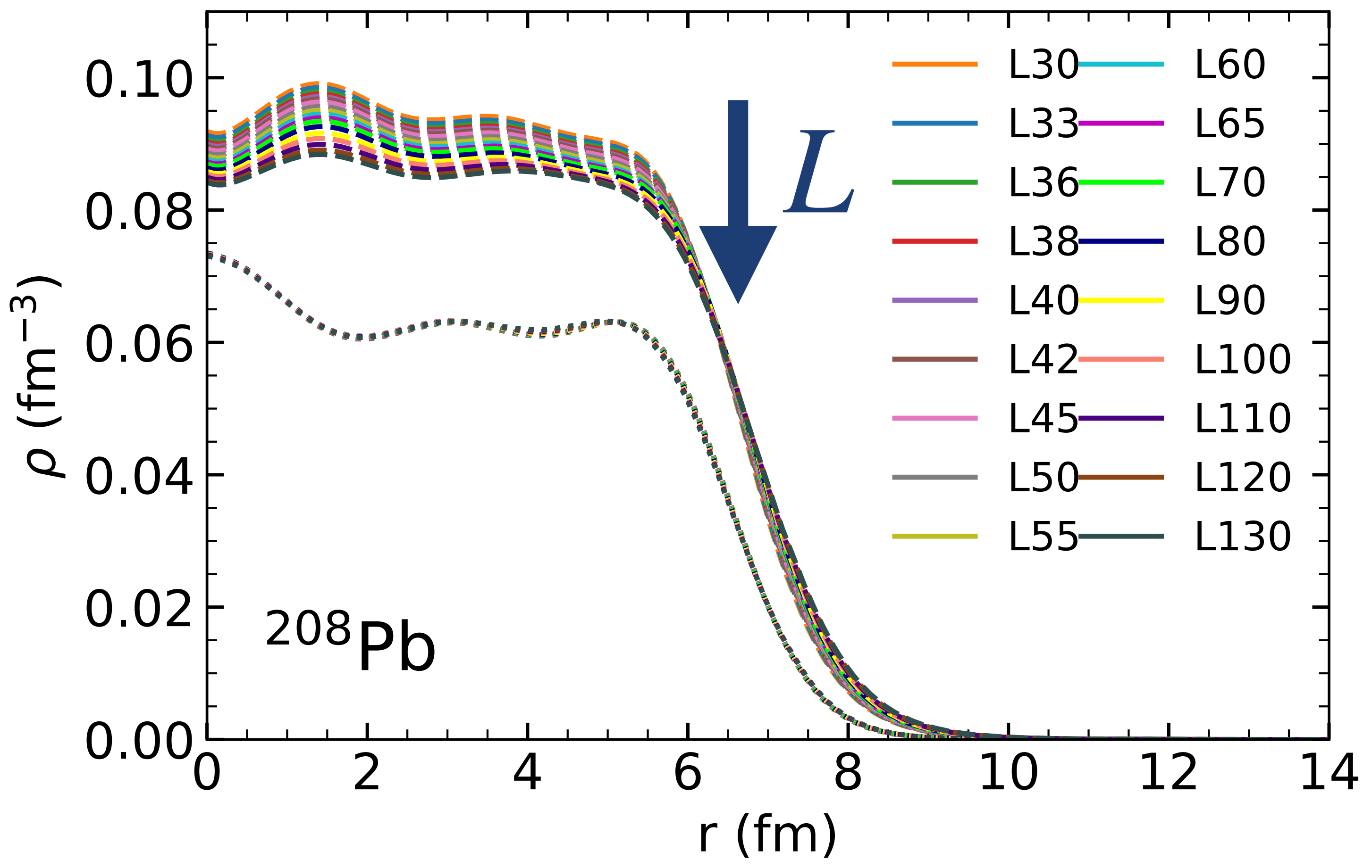

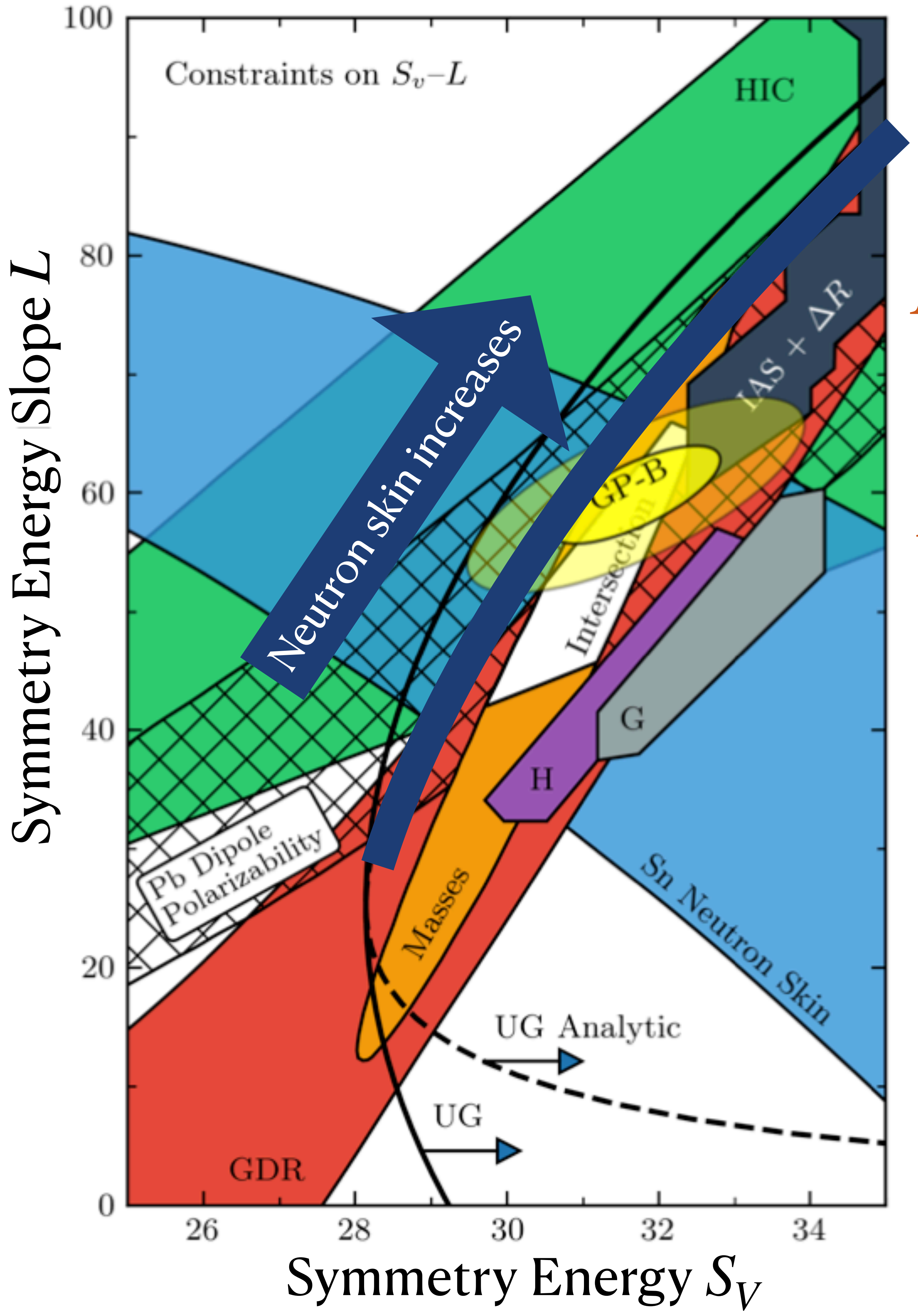

$$E(n_B, x) \approx$$

$$E_{SNM}(u) + E_{SYM}(u)\,(1-2x)^2 + \ldots$$

$$BE + \frac{K}{18}(u-1)^2 + \ldots$$

$$S_v + \frac{L}{3}(u-1) + \frac{K_{SYM}}{18}(u-1)^2 + \ldots$$

Neutron Skin $\Delta R = R_n - R_p$
is "**perpendicular**" to others

$L = 30 - 90$ MeV
$\Delta R_{^{208}Pb} = 0.11 - 0.25$ fm

Neutron skin experiments

Credit: Michaela Thiel

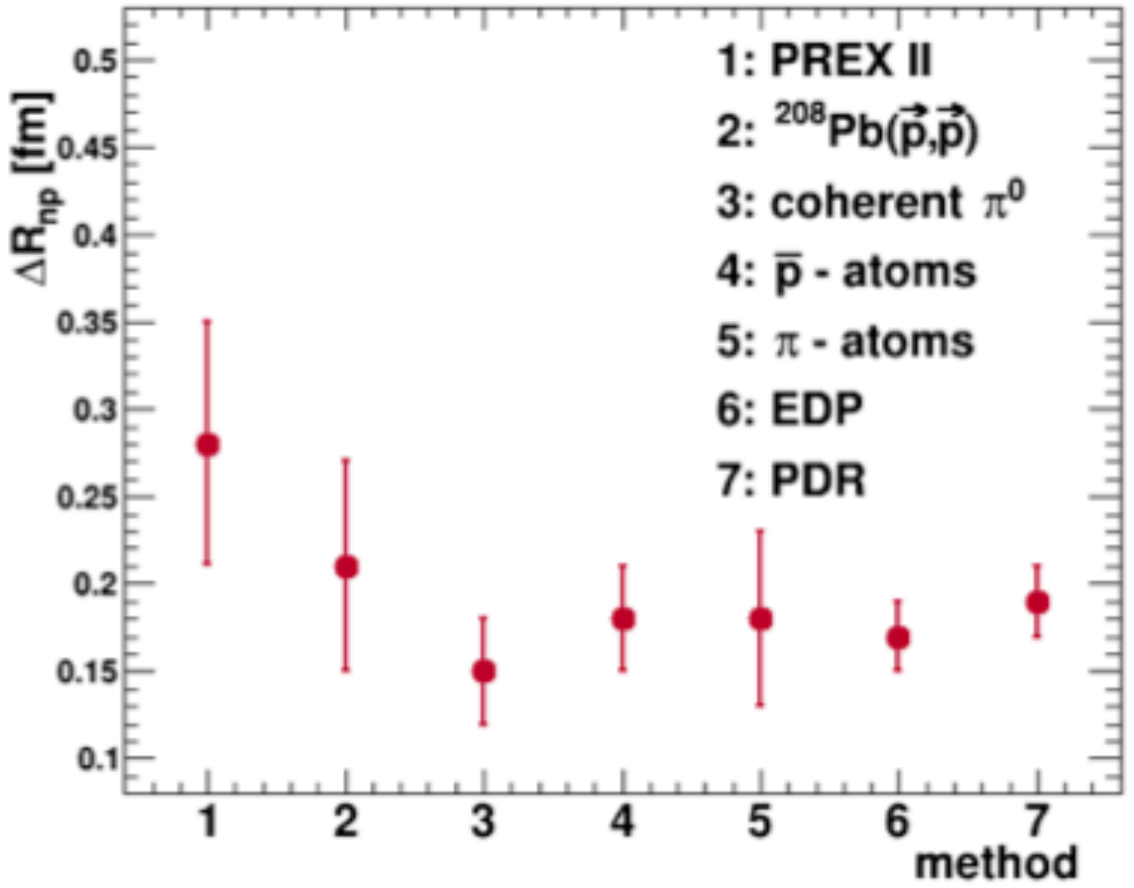

B.T. Reed et al., PRL 126 (2021) 172503

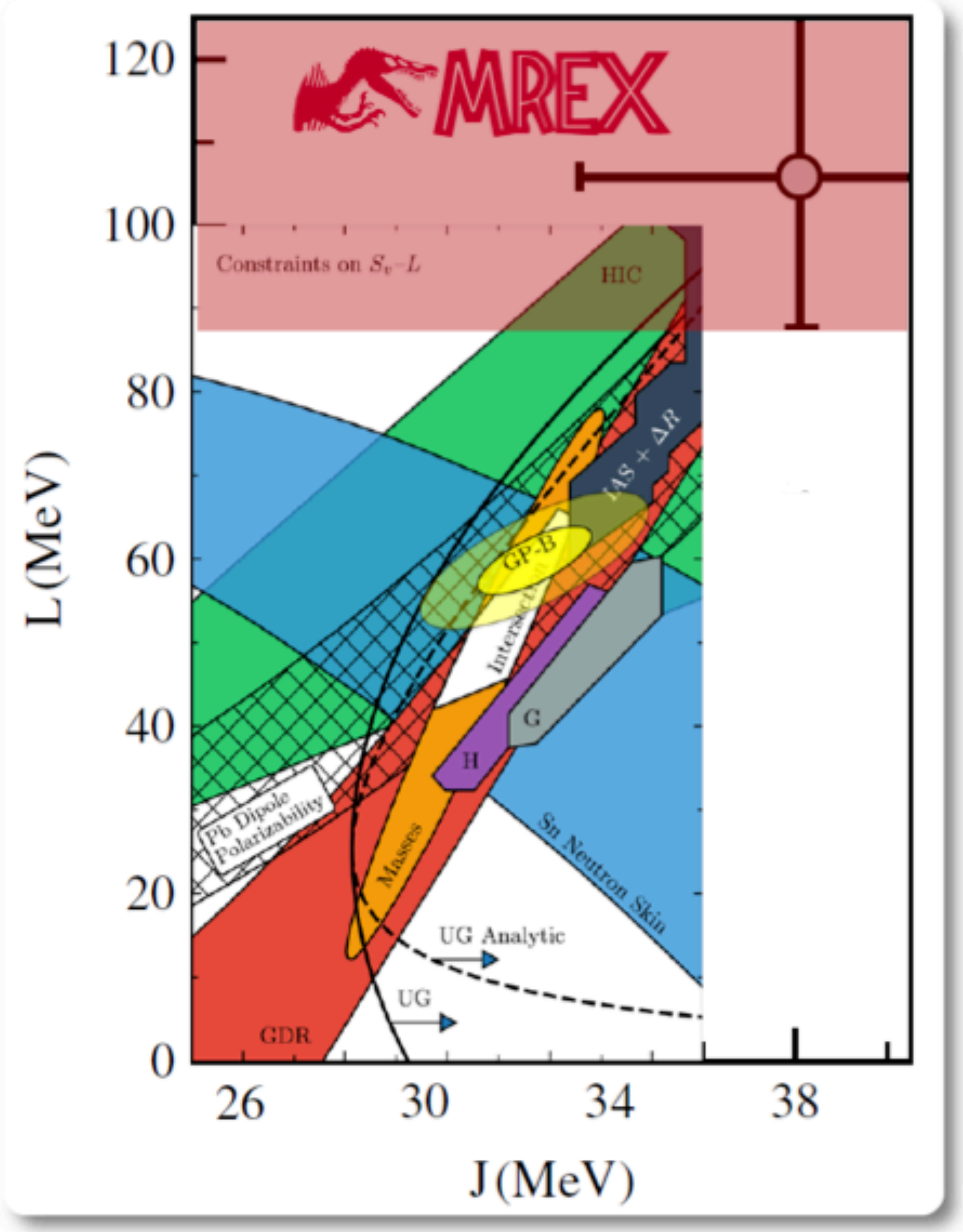

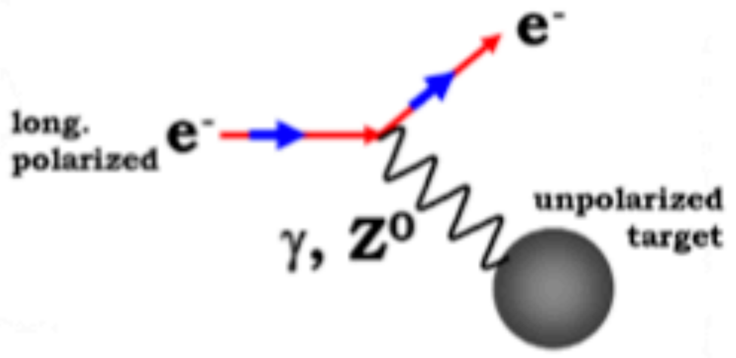

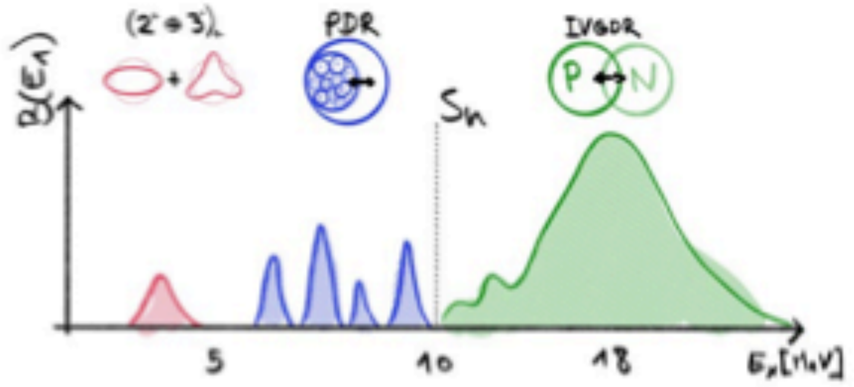

Experimental Challenges (in unit of frustration)

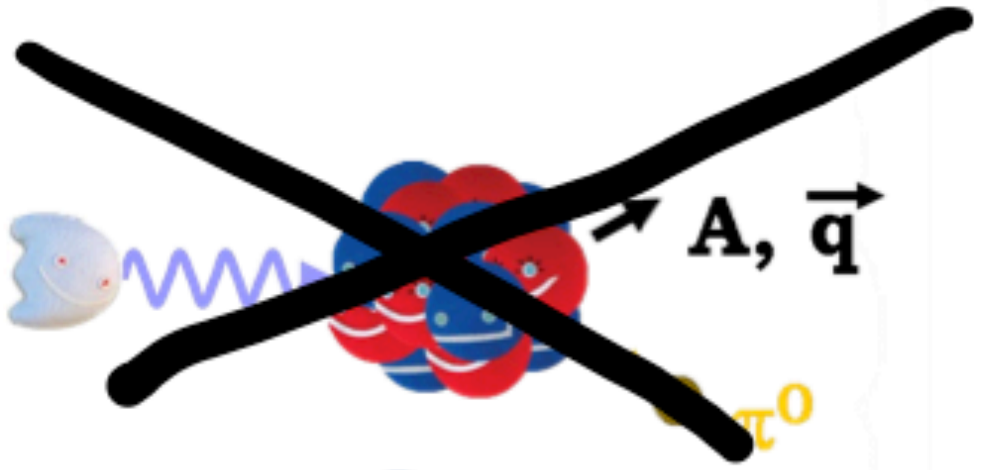

Theo. uncertainties (a.u)

Parity violating electron scattering

	CREX	PREX
(N,Z)	(28,20) Ca	(126,82) Pb
q (fm-1)	0.8733	0.3977
Fch, Rch(fm)	0.1581, 3.481	0.409, 5.503
Apv	2668±106(stat) ±40(syst)	550±16(stat) ±8(syst)
Fw	0.1304±0.0052(stat)±0.002(syst)	0.368±0.013(exp) ±0.001(theo)
Fch-Fw	0.0277±0.0052(stat)±0.002(syst)	0.041±0.013(exp) ±0.001(theo)
Rw	3.64±0.026(exp) ±0.023(theo)	5.8±0.075(tot)
Rw-Rch	0.159±0.026(exp) ±0.023(theo)	0.297±0.075(tot)
Rn-Rp	0.121±0.026(exp) ±0.024(theo)	0.283±0.071(tot)

CREX 2022 PREX I 2012 PREX II 2021

MREX: 208Pb at different momentum q (expected 2030)

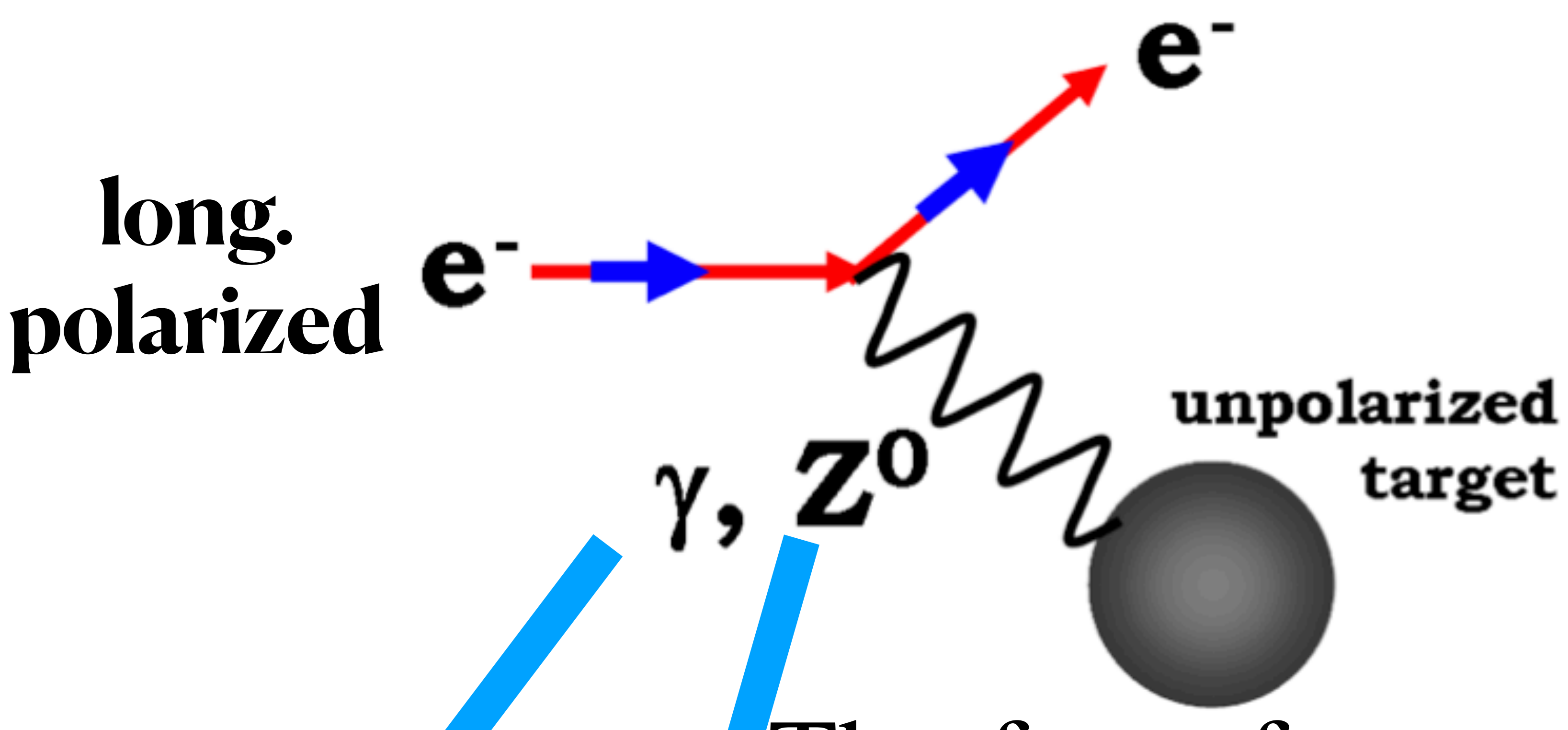

The form factors

$$F_{ch} - F_W = \Delta F$$

Bohn approx.
“back-up slide”

The parity violating asymmetry :

$$A_{PV} = \frac{\sigma_R - \sigma_L}{\sigma_R + \sigma_L}$$

The weak interaction violates parity :

$$J^\mu_Z = -\frac{1}{2}\bar{\psi}_L \gamma^\mu \psi_L - \sin^2(\Theta)\bar{\psi}\gamma^\mu\psi$$

OUTLINE

- Nuclear models
- Symmetry energy & Neutron skin experiments (PREX & CREX)
- Tensions between PREX+CREX and mean field models
- Constraints on bulk properties (symmetry energy)
- Constraints on surface properties (spin-orbit coupling)
- Takeaways

Pre PREX-CREX era

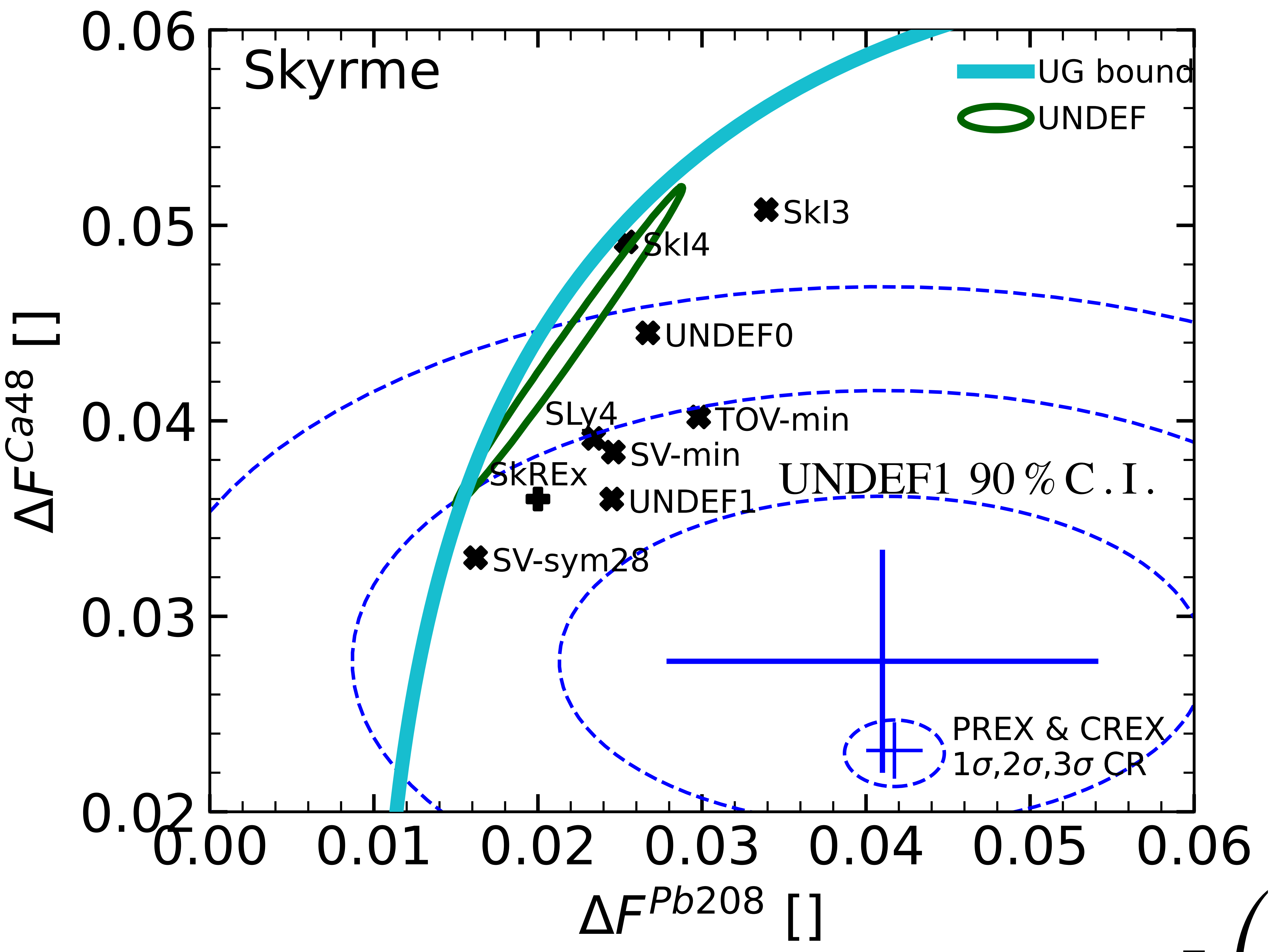

Pre PREX-CREX era models

$$\bar{\psi}\left(\frac{g_\delta}{2}\tau \cdot \delta\right)\psi$$

Pre PREX-CREX era

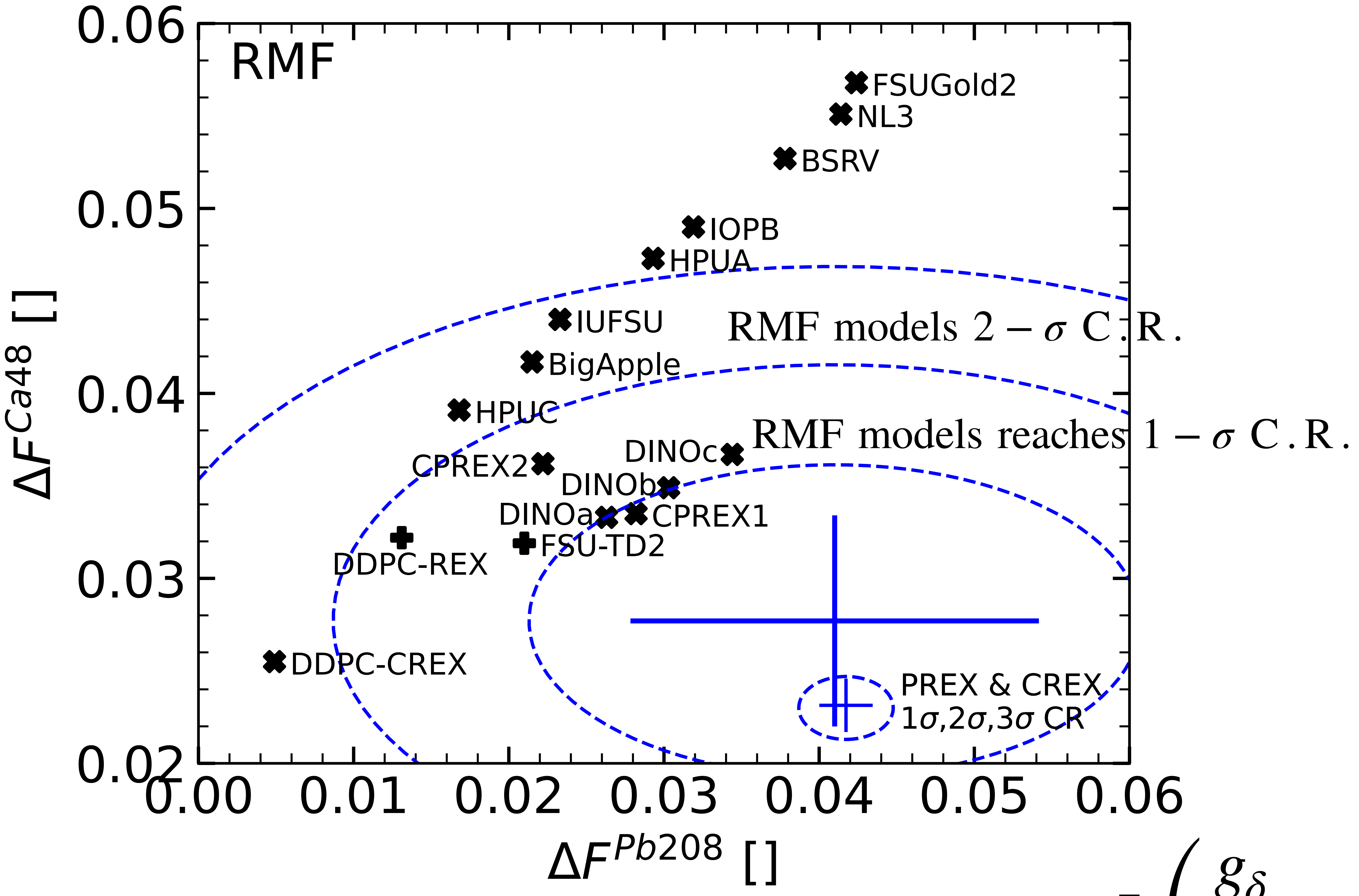

$$\bar{\psi}\left(\frac{g_\delta}{2}\tau\cdot\delta\right)\psi$$

+Post PREX-CREX era models with delta-meson interaction

Post PREX-CREX era

- What nuclear properties can we learn from the experiment?
- Why are Skyrme models more compatible than RMF models?
- How may the mean-field model improve in the future?

OUTLINE

- Nuclear models
- Symmetry energy & Neutron skin experiments (PREX & CREX)
- Tensions between PREX+CREX and mean field models
- Constraints on bulk properties (symmetry energy)
- Constraints on surface properties (spin-orbit coupling)
- Takeaways

Skyrme and RMF samples

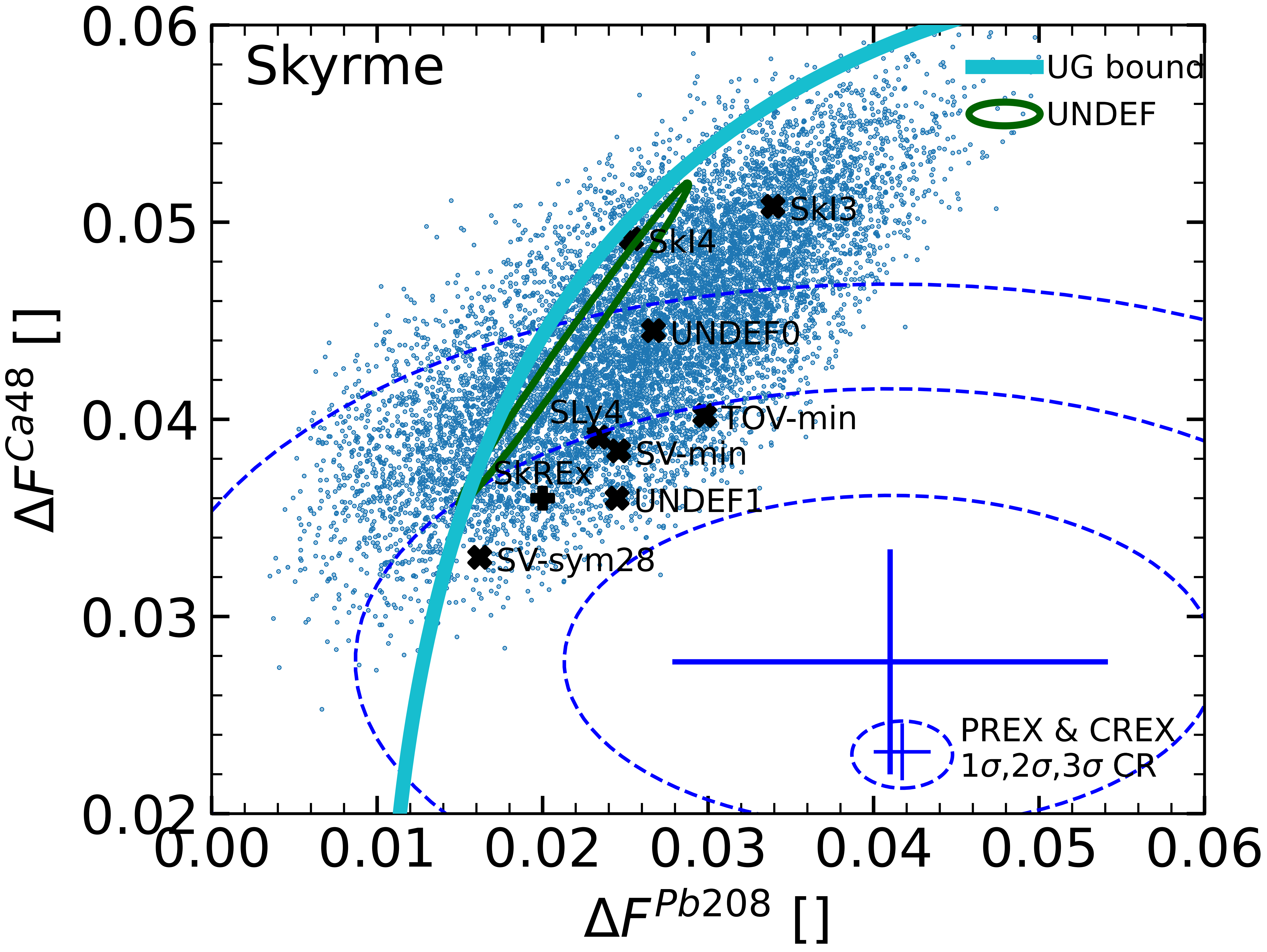

Skyrme models

Skyrme and RMF samples

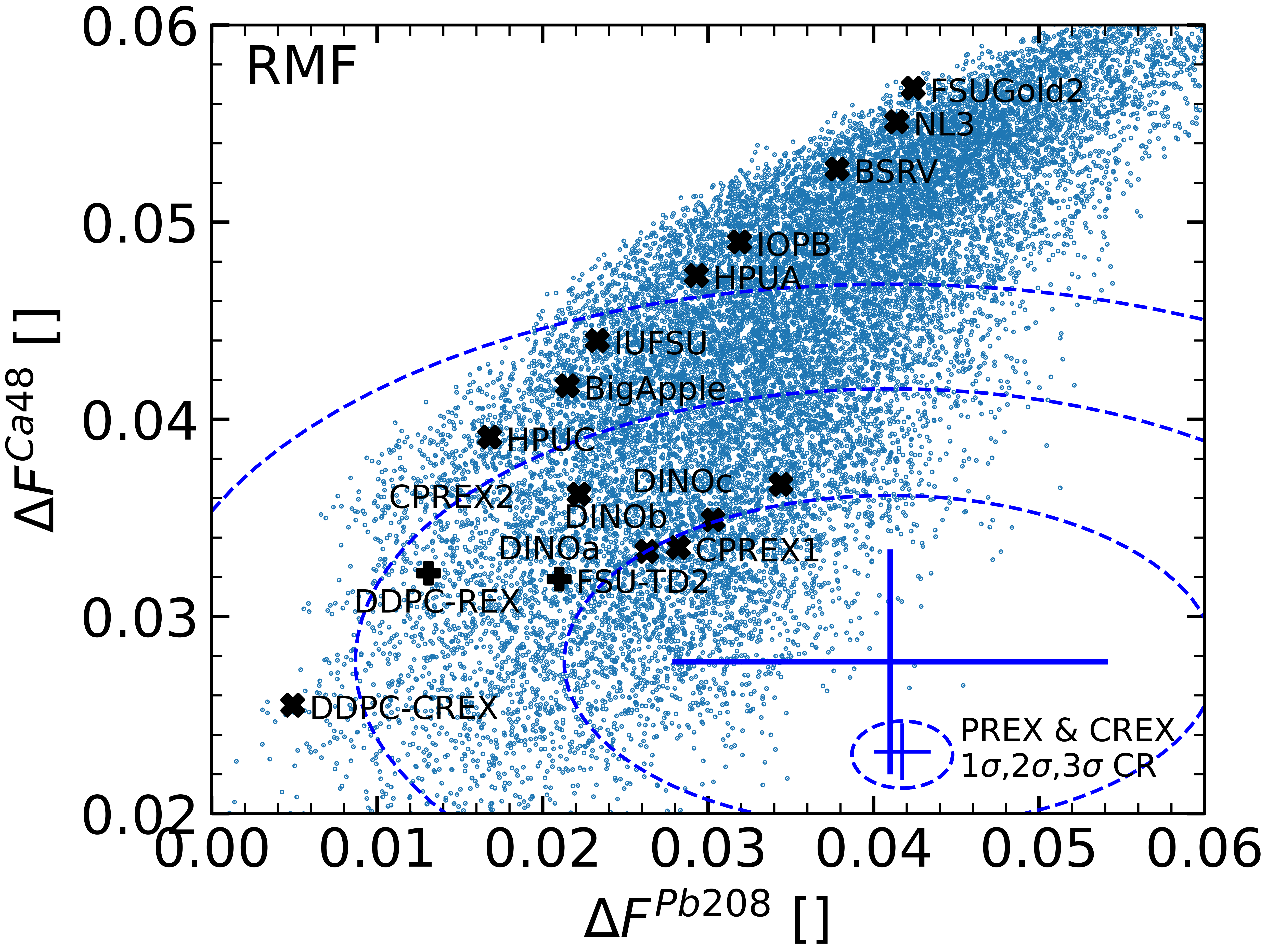

RMF models

Symmetry energy S_V

$$S(n) = S_V + \frac{L}{3}(\frac{n}{n_S} - 1) + \cdots$$

- ΔF^{Ca48} and ΔF^{Pb208} are positively correlated for nuclear models with fixed S_V
- The correlation is linear: $S_v = a\Delta F^{Ca48} + b\Delta F^{Pb208} + c$
- Fitting parameter for RMF (Skyrme) models:

	a	b	c
RMF	-575.2 ± 5.1	916.3 ± 4.6	32.2 ± 3.7
Skyrme	-503.2 ± 7.8	945.2 ± 5.5	31.9 ± 2.9

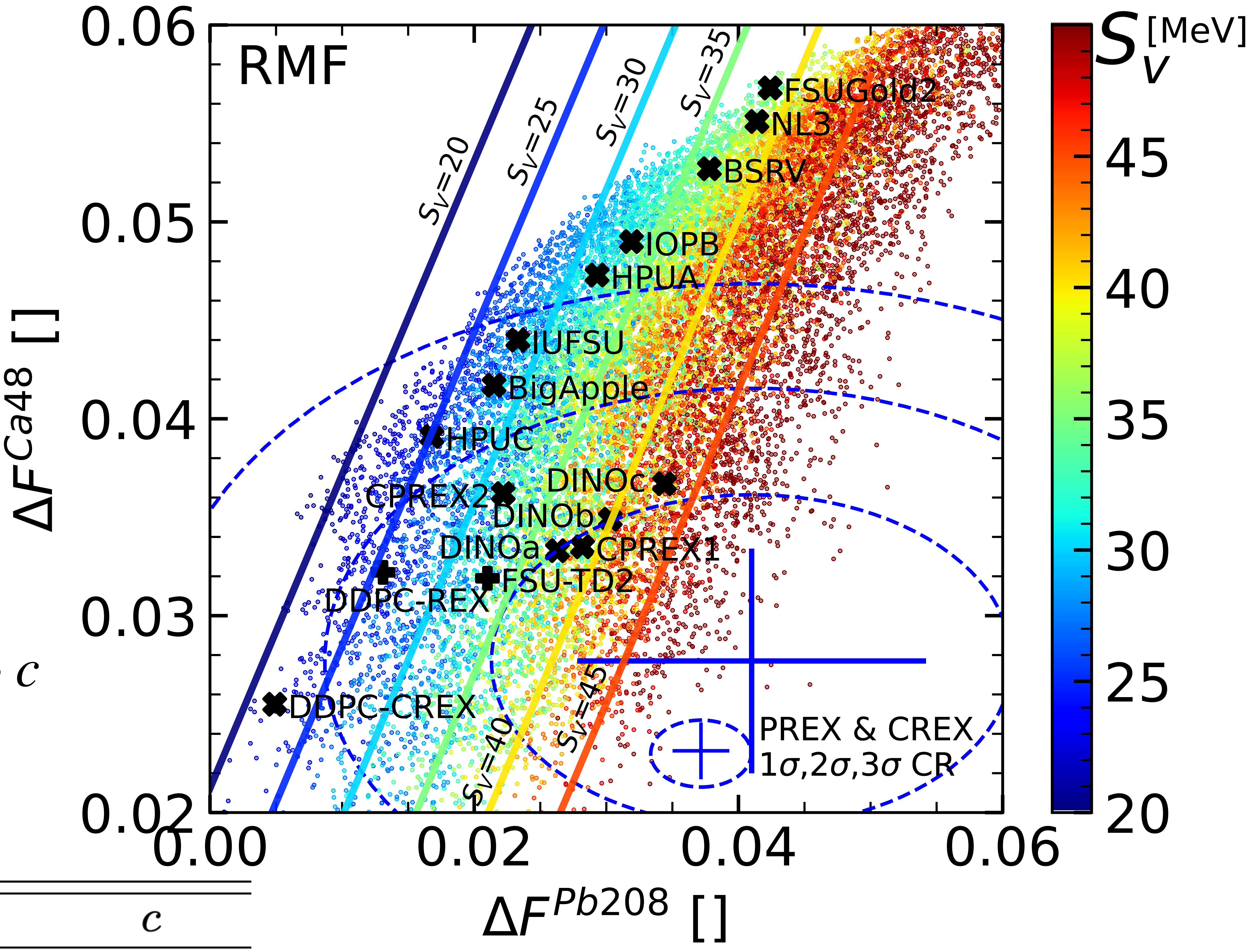

Linear correlation of form factor difference

Symmetry energy slope L

$$S(n) = S_V + \frac{L}{3}\left(\frac{n}{n_S} - 1\right) + \cdots$$

- A similar correlation for L has an opposite slope!
- The correlation is linear: $L = a'\Delta F^{Ca48} + b'\Delta F^{Pb208} + c'$
- Fitting parameter for RMF (Skyrme) models:

	a'	b'	c'
RMF	2938.7 ± 43.5	2420.6 ± 33.9	-149.8 ± 25.6
Skyrme	1791.2 ± 27.2	2652.0 ± 19.0	-91.5 ± 10.1

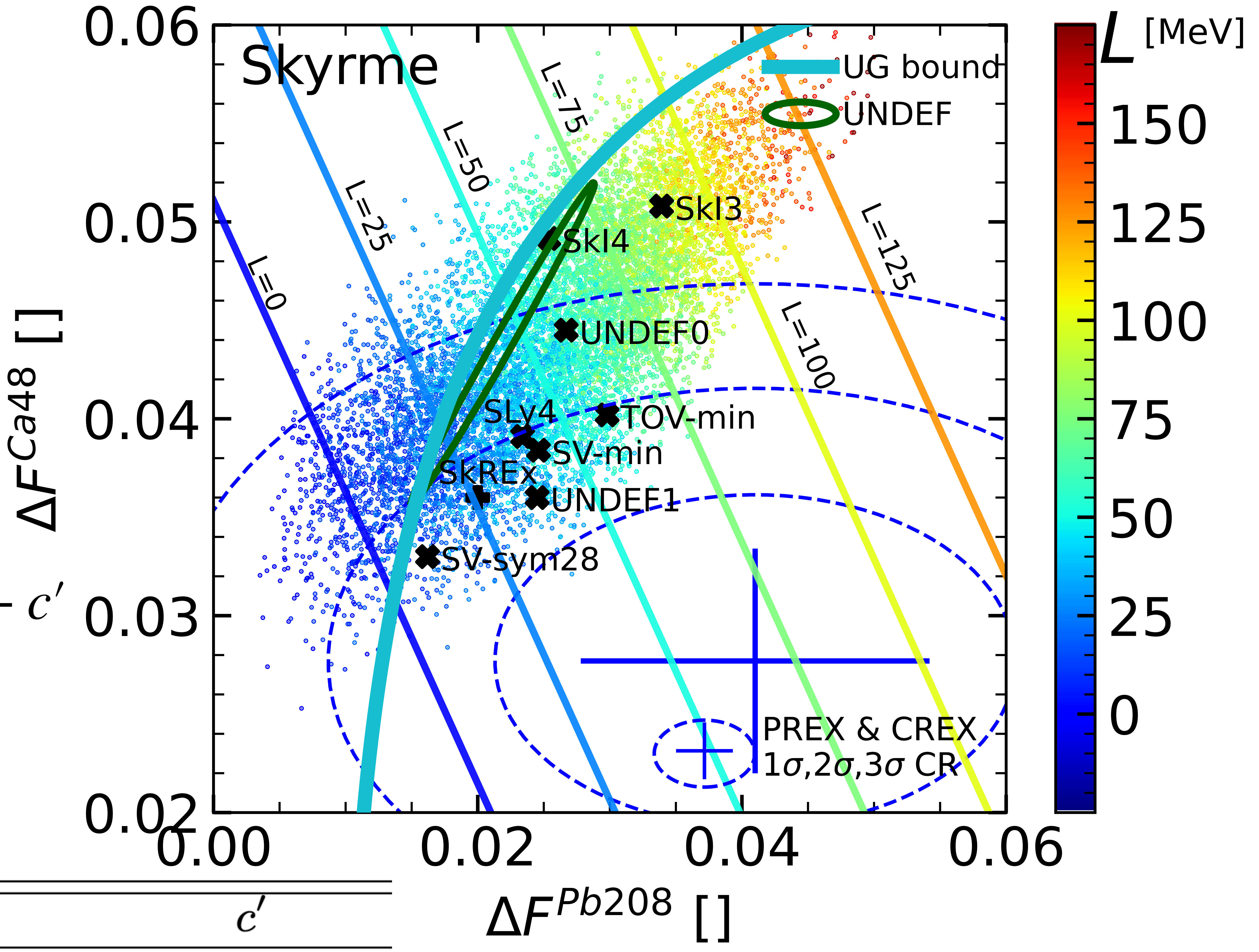

Linear correlation of form factor difference

Constraints on (S_V , L) from (ΔF^{Ca48},ΔF^{Pb208})

- S_V and L can be fixed by ΔF^{Ca48} and(or) ΔF^{Pb208}:
  $S_V = a\Delta F^{Ca48} + b\Delta F^{Pb208} + c$
  $L = a'\Delta F^{Ca48} + b'\Delta F^{Pb208} + c'$
- PREX:
  ΔF^{Pb208}=0.041
  ±0.013(exp)±0.001(theo)
- CREX:
  ΔF^{Ca48}=0.0277
  ±0.0052(stat)±0.002(syst)
- PREX+CREX:

$$(\bar{S}_{\rm V}, \bar{L}) \;=\; (56.7,\;\; 66.8)_{Skyrme},\quad (53.8,\;\; 30.9)_{RMF}$$

$$\sqrt{\rm cov} \;=\; \begin{pmatrix} 19.6 & 31.2 \\ 31.2 & 56.5 \end{pmatrix}_{Skyrme},\quad \begin{pmatrix} 19.5 & 31.0 \\ 31.0 & 66.3 \end{pmatrix}_{RMF}$$

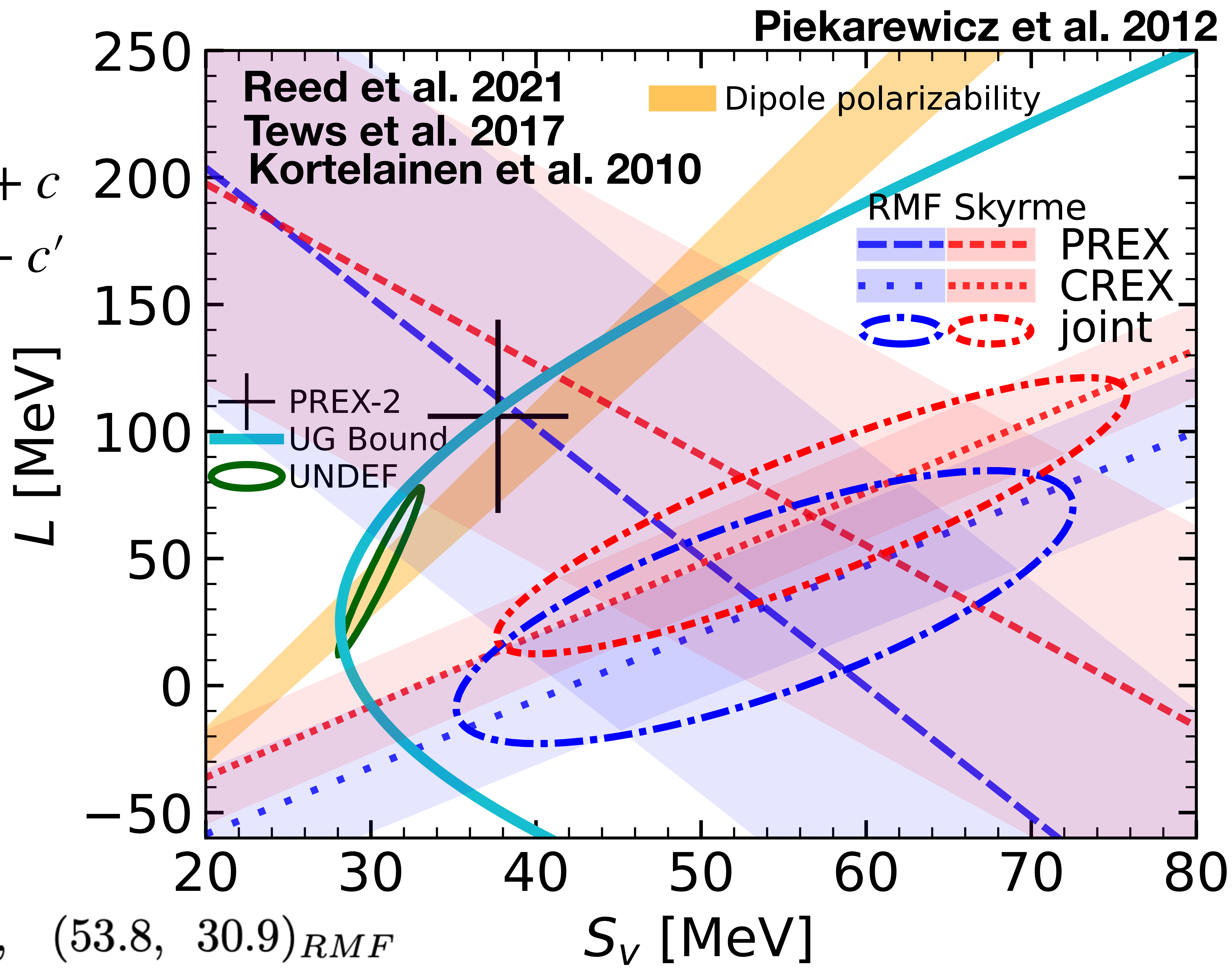

Compare with prior knowledge of Sv and L

Bayesian posterior

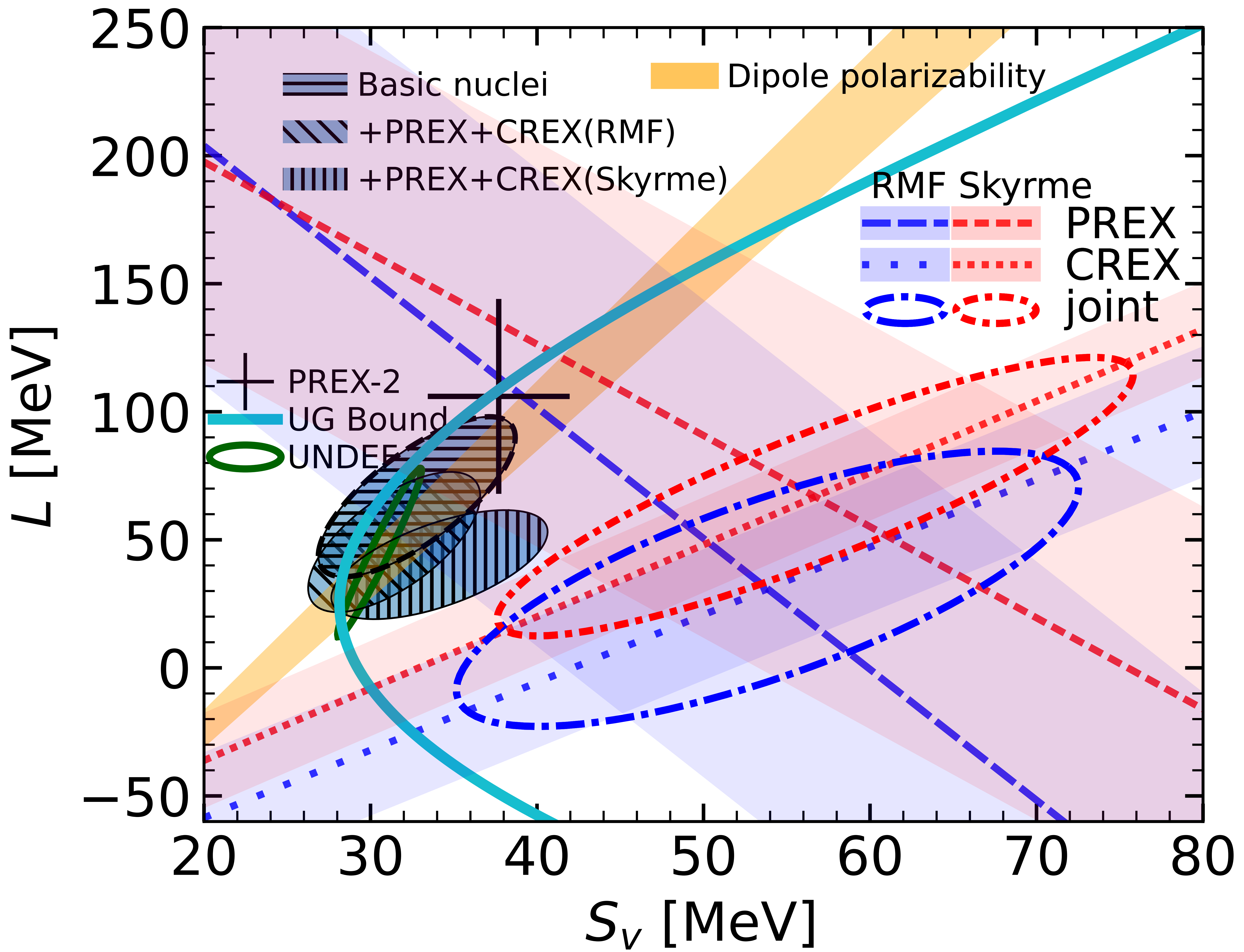

OUTLINE

- Nuclear models
- Symmetry energy & Neutron skin experiments (PREX & CREX)
- Tensions between PREX+CREX and mean field models
- Constraints on bulk properties (symmetry energy)
- Constraints on surface properties (spin-orbit coupling)
- Takeaways

Isovector spin-orbit force

- Isovector spin-orbit force is independent of S_V and L in Skyrme (not in RMF) model.
- Spin-orbit force in Skyrme model:
  $H_{\mathrm{SO}} = b_4 \mathrm{J} \cdot \nabla n$
  $+ b_4'(\mathrm{J}_n \cdot \nabla n_n + \mathrm{J}_p \cdot \nabla n_p)$
  The freedom b_4' improves the Skyrme model performance.
- $v \ll c$ limit of RMF model:
  $$b_4' \approx \frac{1}{8m^2}\left(\frac{g_\delta^2}{m_\delta^2} + \frac{g_\rho^2}{m_\rho^2}\right)$$
  large δ-meson coupling improves the RMF models.

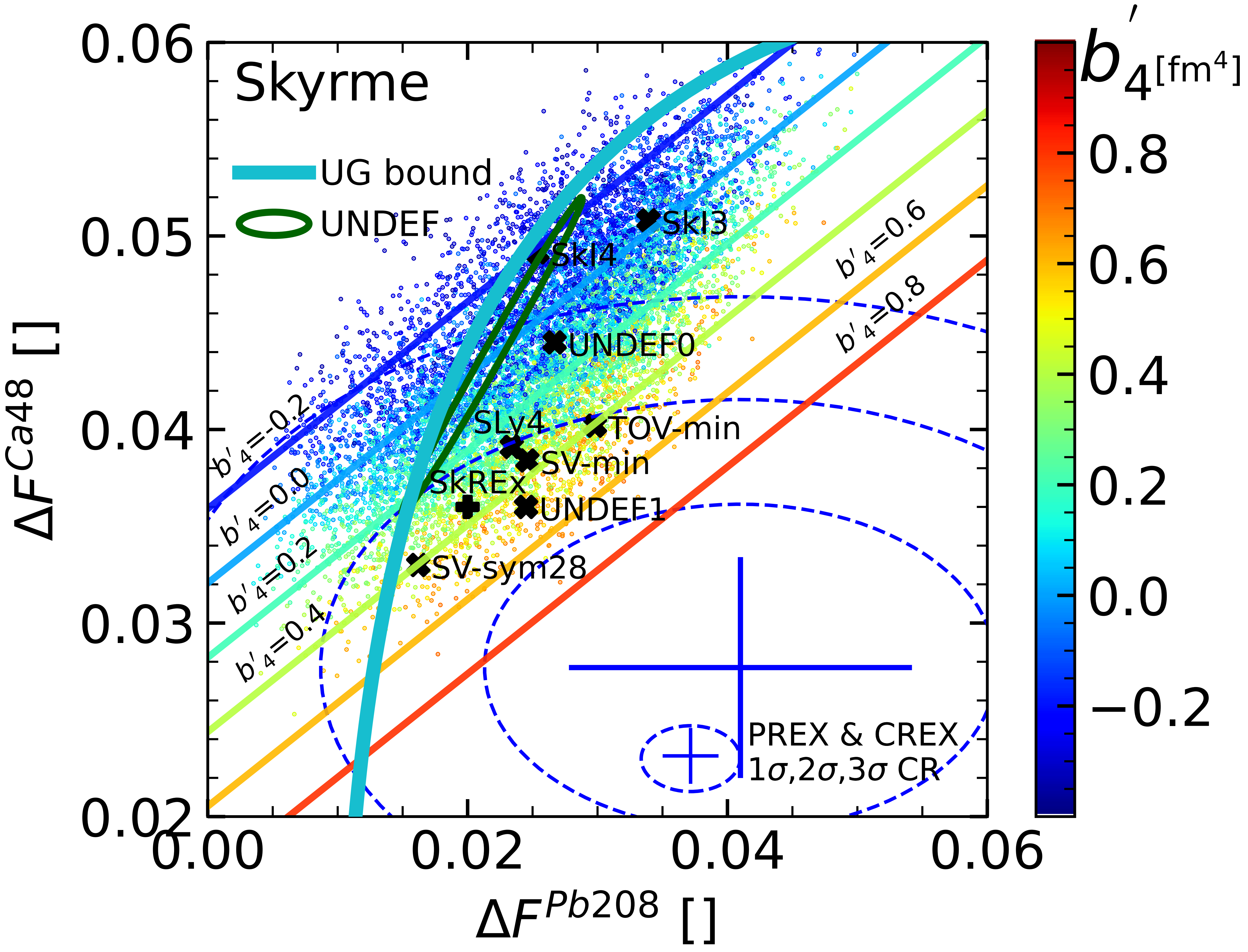

Linear correlation of form factor difference

Isovector spin-orbit force

- Isovector spin-orbit force is independent of S_V and L in Skyrme (not in RMF) model.
- Spin-orbit force in Skyrme model:
  $H_{\mathrm{SO}} = b_4 \mathrm{J} \cdot \nabla n$
  $+ b_4'(\mathrm{J}_n \cdot \nabla n_n + \mathrm{J}_p \cdot \nabla n_p)$
  The freedom b_4' improves the Skyrme model performance.
- $v \ll c$ limit of RMF model:
  $$b_4' \approx \frac{1}{8m^2}\left(\frac{g_\delta^2}{m_\delta^2} + \frac{g_\rho^2}{m_\rho^2}\right)$$
  large δ-meson coupling improves the RMF models.

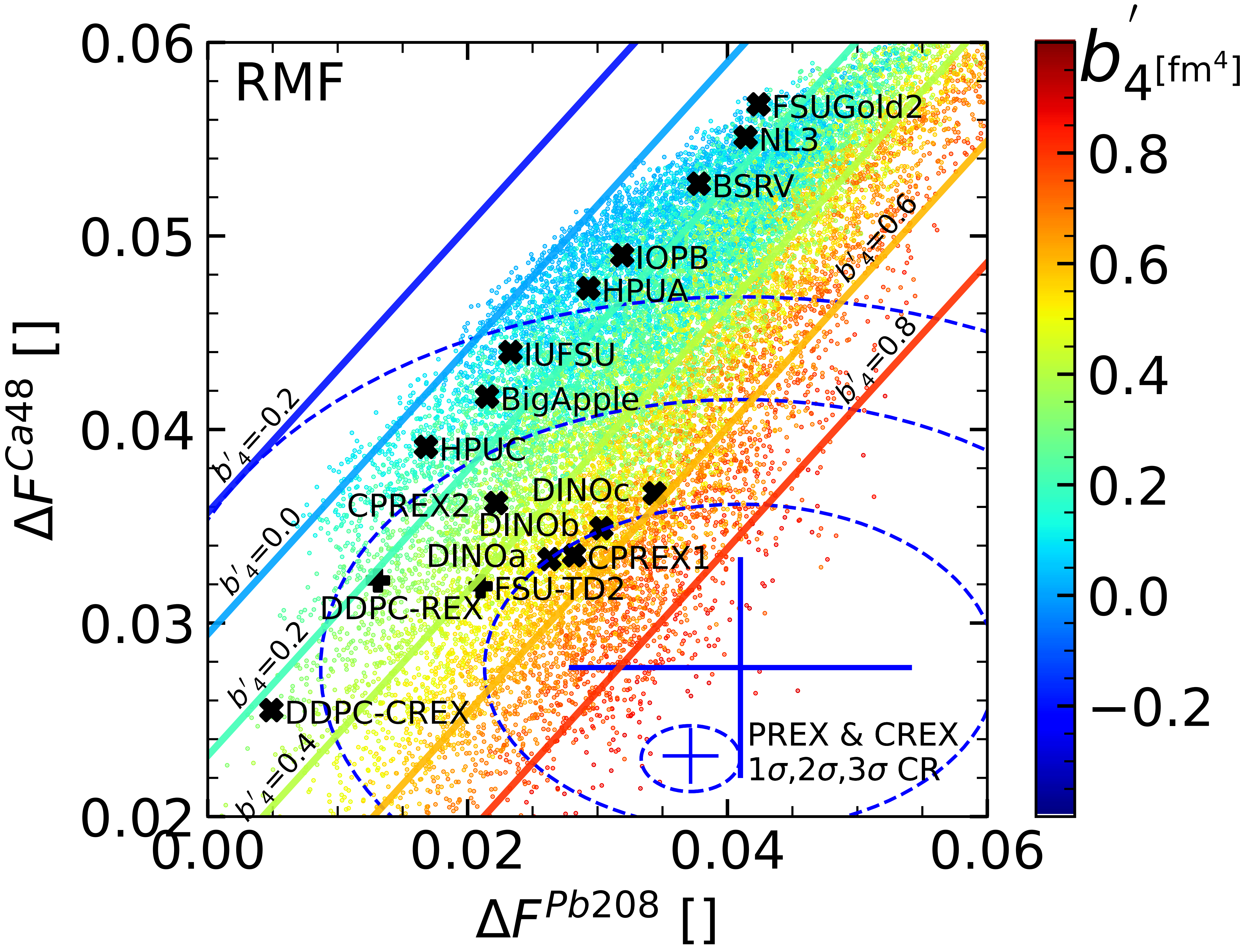

Linear correlation of form factor difference

Impact of b_4' on neutron skin ΔR_{np}

- ΔR_{np} of ^{208}Pb increases with b_4'
- ΔR_{np} of ^{48}Ca decreases with b_4'
- Large b_4' reduces the tension between PREX and CREX.
- 90% lower bound of b_4':
  $b_4' \gtrsim 0.74\ \mathrm{fm}^4$ (Skyrme)
  $b_4' \gtrsim 0.54\ \mathrm{fm}^4$ (RMF)
- The large density fluctuation inside nuclei may be reduced by introducing addition tensor interactions, see M. Salinas and J. Piekarewicz 2024 (arXiv:2312.13474)

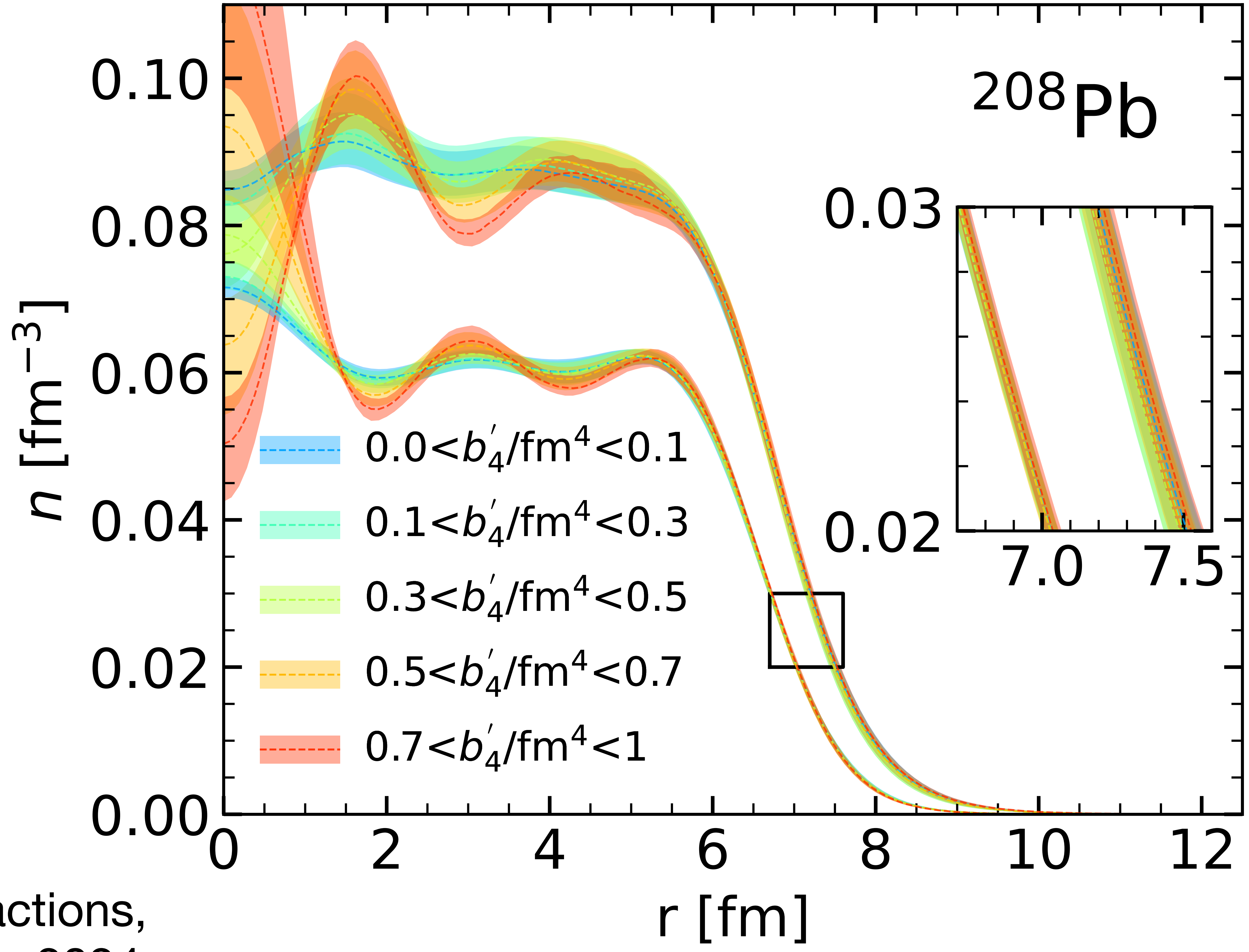

Radial density profile of proton and neutron for 208Pb

Impact of b_4' on neutron skin ΔR_{np}

- ΔR_{np} of ^{208}Pb increases with b_4'
- ΔR_{np} of ^{48}Ca decreases with b_4'
- Large b_4' reduces the tension between PREX and CREX.
- 90% lower bound of b_4':
  $b_4' \gtrsim 0.74\ \mathrm{fm}^4$ (Skyrme)
  $b_4' \gtrsim 0.54\ \mathrm{fm}^4$ (RMF)
- The large density fluctuation inside nuclei may be reduced by introducing addition tensor interactions, see M. Salinas and J. Piekarewicz 2024 (arXiv:2312.13474)

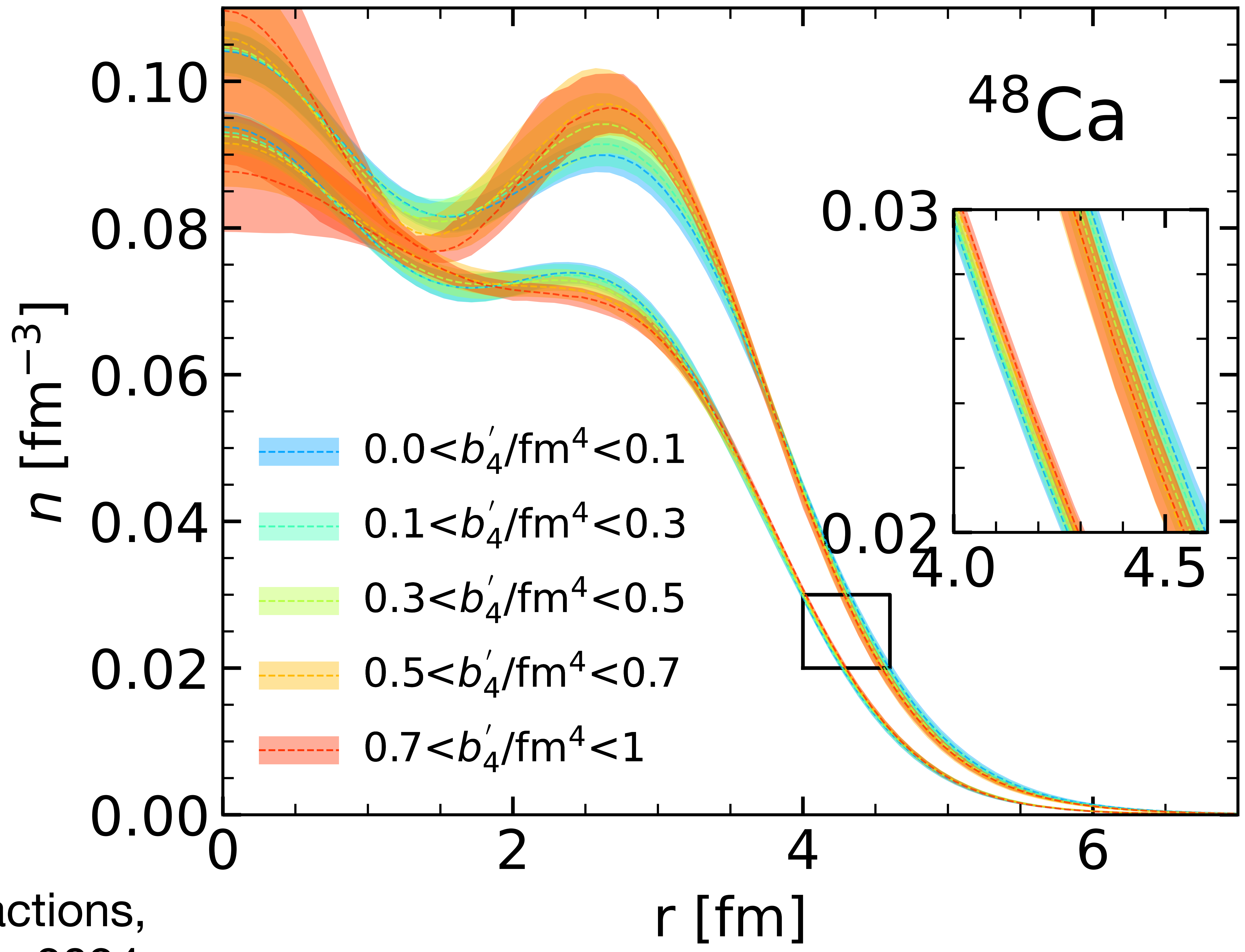

Radial density profile of proton and neutron for 48Ca

Impact of b'_4 on neutron skin ΔR_{np}

- ΔR_{np} of ^{208}Pb increases with b'_4
- ΔR_{np} of ^{48}Ca decreases with b'_4
- Large b'_4 reduces the tension between PREX and CREX.
- 90% lower bound of b'_4:
  $b'_4 \gtrsim 0.74\ \mathrm{fm}^4$ (Skyrme)
  $b'_4 \gtrsim 0.54\ \mathrm{fm}^4$ (RMF)
- The large density fluctuation inside nuclei may be reduced by introducing addition tensor interactions, see M. Salinas and J. Piekarewicz 2024 (arXiv:2312.13474)

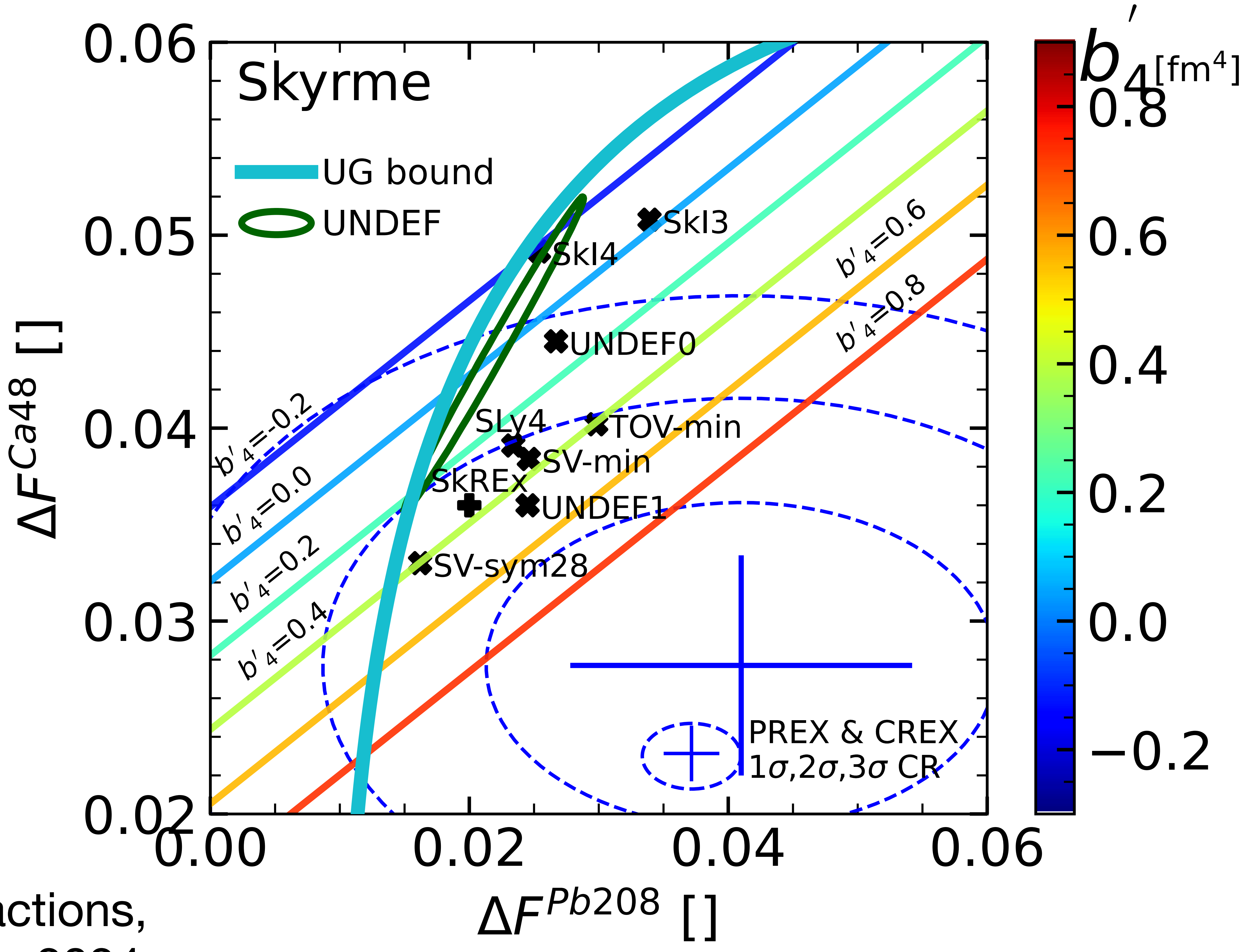

Linear correlation of form factor difference with fixed b'4

Impact of b_4' on neutron skin ΔR_{np}

- ΔR_{np} of ^{208}Pb increases with b_4'
- ΔR_{np} of ^{48}Ca decreases with b_4'
- Large b_4' reduces the tension between PREX and CREX.
- 90% lower bound of b_4':
  $b_4' \gtrsim 0.74\ \mathrm{fm}^4$ (Skyrme)
  $b_4' \gtrsim 0.54\ \mathrm{fm}^4$ (RMF)
- The large density fluctuation inside nuclei may be reduced by introducing addition tensor interactions, see M. Salinas and J. Piekarewicz 2024 (arXiv:2312.13474)

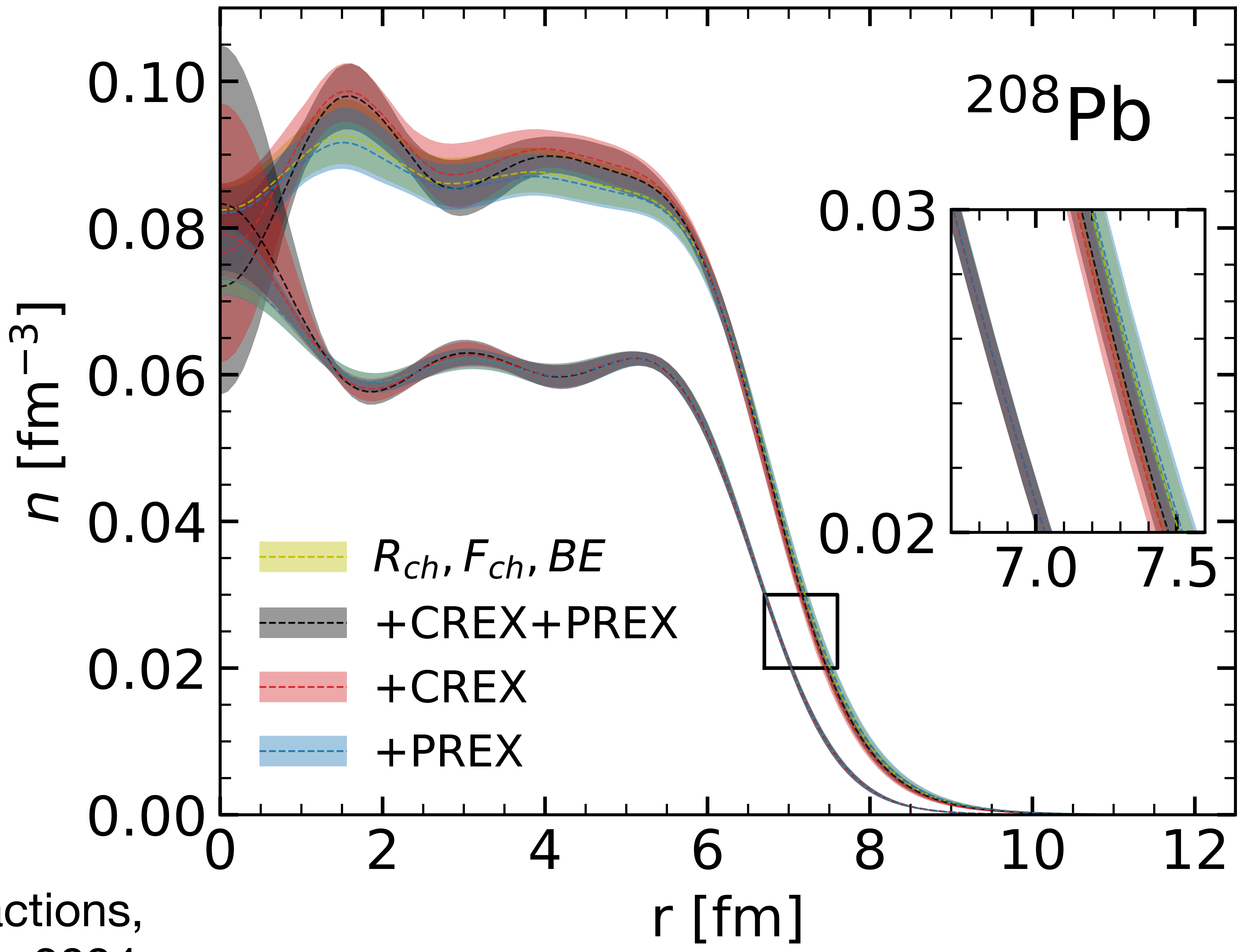

Bayesian posterior prefers large density fluctuation

Free Tensor Interaction

- Spin-orbit force in Skyrme model:
  $H_{\mathrm{SO}} = b_4 \mathrm{J} \cdot \nabla n$
  $+ b_4' (\mathrm{J}_n \cdot \nabla n_n + \mathrm{J}_p \cdot \nabla n_p)$
  Tensor force in Skyrme model:
  $H_{\mathrm{T}} = b_J \mathrm{J}^2 + b_J' (\mathrm{J}_n^2 + \mathrm{J}_p^2)$
  The freedom b_4', b_4' and b_4'improve the Skyrme model performance, see arXiv.2406.03844:
  S240 and eS240: $b_4' = 0.6\ \mathrm{fm}^{-4}$
  S500 and eS500: $b_4' = 1.3\ \mathrm{fm}^{-4}$

- which is consistent with our analysis:
  $b_4' = 1.37 \pm 0.49\ \mathrm{fm}^{-4}$
  and 90% lower bound:
  $b_4' \gtrsim 0.74\ \mathrm{fm}^4$ (Skyrme)
  $b_4' \gtrsim 0.54\ \mathrm{fm}^4$ (RMF)

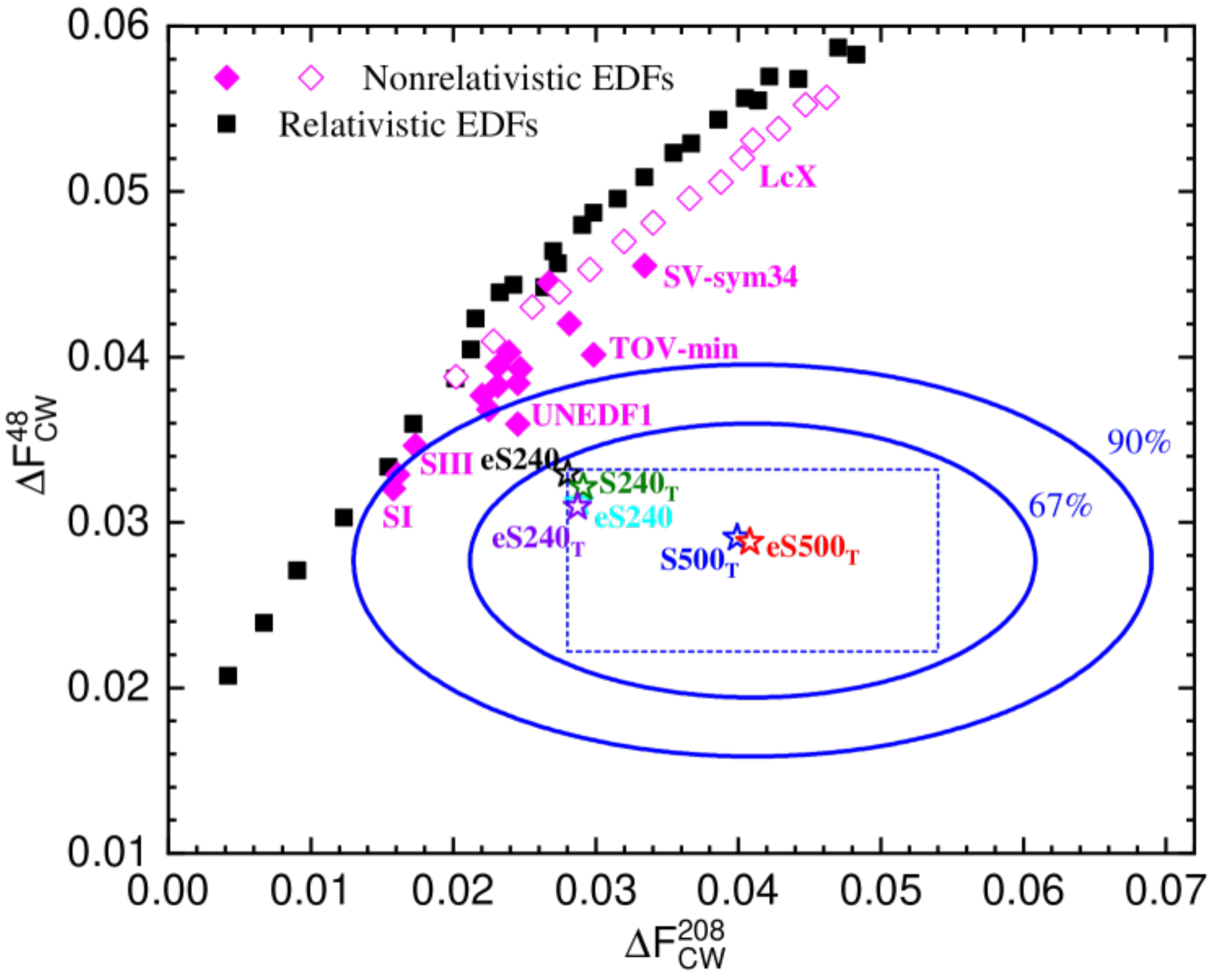

T.G. Yue, Z. Zhang, L.W. Chen arXiv.2406.03844

Take away

- What nuclear properties can we learn from the experiment?
  PREX+CREX prefers much Larger S_V than expected.

- Why are Skyrme models more compatible than RMF models?
  The freedom in isovector spin-orbit interaction b_4'.

- How may the mean-field model improve in the future?
  Increase the degree of freedom on surface-related isovector interactions, e.g. isovector spin-orbit interaction, isovector tensor interaction.

see arXiv.2406.05267

Tianqi Zhao, Zidu Lin, Bharat Kumar, Andrew Steiner, Madappa Prakash

Back up slides


Neutron star radius
Bulk nuclear matter properties
Neutron skin of closed shell nucleus
Neutral current interaction
Weak form factor
Neutron(weak) radius
Unified description
Static field
Dirac EQ
Coulomb distortion
Parity violation asymmetry
Coulomb interaction
Electric form factor
Born approximation
Chen 2010
Reed 2021
PREX I 2012
CREX 2022
Reinhard 2021
Horowitz 2000
Horowitz 1998
Lin 2015
Steiner 2005
PREX II 2021

Back

QED and Weak interaction

- Lagrange involving electron:

$$\mathscr{L} = \mathbf{i}\bar{\psi}\gamma^\mu\partial_\mu\psi - m\bar{\psi}\psi + eJ^\mu A_\mu + \frac{g_W}{\cos(\Theta_W)}J_Z^\mu Z_\mu - \frac{M_Z^2}{2}Z^\mu Z_\mu + \dots$$

$J^\mu = (\rho_E, \mathbf{j}) = \bar{\psi}\gamma^\mu\psi$ is electron 4-current,

and $J_Z^\mu = -\frac{1}{2}\bar{\psi}_L\gamma^\mu\psi_L - \sin^2(\Theta)\bar{\psi}\gamma^\mu\psi = -\frac{1}{4}\bar{\psi}\left[1 - 4\sin^2(\Theta_W) - \gamma^5\right]\psi$

Weak mixing angle: $\cos(\Theta_W) = \frac{M_W}{M_Z} = 0.882$

$M_W = 80.4\ \mathrm{GeV},\ \ M_Z = 91.2\ \mathrm{GeV},\ \ \sin^2(\Theta_W) = 0.223$

- Z boson propagator: $\frac{g_{\mu\nu}}{M_Z^2 - q^2}$

- 4-Fermi effective interaction at zero momentum : $G_F = \frac{g_W^2}{4\sqrt{2}M_W^2}$

Back

Maxwell Equations of E.M. and Weak fields

- Lagrange involving photon and Z boson:

$$\mathscr{L} = \left[-\frac{1}{4}F^{\mu\nu}F_{\mu\nu} + eJ^{\mu}A_{\mu}\right] + \left[-\frac{1}{4}Z^{\mu\nu}Z_{\mu\nu} + \frac{g_W}{\cos(\Theta_W)}J_Z^{\mu}Z_{\mu} - \frac{1}{2}M_Z^2Z^{\mu}Z_{\mu}\right]$$

where $F_{\mu\nu} = \partial^{\mu}A_{\nu} - \partial^{\nu}A_{\mu}, Z_{\mu\nu} = \partial^{\mu}Z_{\nu} - \partial^{\nu}Z_{\mu}$

$A_{\mu} = (\Phi, \mathbf{A}), Z_{\mu} = (\Phi_Z, \mathbf{Z})$ are gauge boson fields,

and $J^{\mu} = (\rho_E, \mathbf{j}) = \bar{\psi}\gamma^{\mu}\psi$ is E.M. 4-current of an electron.

- E.M. field follows Maxwell Equations: $\nabla^2\Phi - \frac{\partial^2\Phi}{\partial_t^2} = \rho_E + (M^2\Phi$ for massive Z boson)

Static electric potential: $\Phi(r) = \int \frac{\rho_E(r')}{4\pi|r-r'|}dr'^3$

Static Z-boson potential: $\Phi_Z(r) = \int \frac{\rho_Z(r')e^{-M_Z|r-r'|}}{4\pi|r-r'|}dr'^3 \approx \rho_Z(r')\int \frac{e^{-M_Z|r-r'|}}{4\pi|r-r'|}dr'^3 = \frac{\rho_Z(r')}{M_Z^2}$

<u>Weak interaction is approximately zero-range, since $M_Z \approx 500$ fm^{-1}</u>

Back

Dirac equation in E.M. and weak field

V-A theory

- Lagrange involving electron:

$$\mathscr{L} = \mathbf{i}\bar{\psi}\gamma^{\mu}\partial_{\mu}\psi - m\bar{\psi}\psi + eJ^{\mu}A_{\mu} + \frac{g_W}{\cos(\Theta_W)}J^{\mu}_{Z}Z_{\mu} - \frac{M_Z^2}{2}Z^{\mu}Z_{\mu} + \ldots$$

- Electron weak 4-current:

$$J^{\mu}_{Z} = -\frac{1}{2}\bar{\psi}_L\gamma^{\mu}\psi_L + \sin^2(\Theta)\bar{\psi}\gamma^{\mu}\psi = -\frac{1}{4}\bar{\psi}\gamma^{\mu}\left[1 - 4\sin^2(\Theta_W) - \gamma^5\right]\psi \approx \frac{1}{4}\bar{\psi}\gamma^{\mu}\gamma^5\psi$$

- Dirac equation: $\left[\alpha\mathbf{p} + \beta m + \hat{V}(r)\right]\Psi = E\psi$

where $\hat{V}(r) = V(r) + \gamma_5 A(r), \;\; V(r) = \int d^3\mathbf{r}'\frac{\rho_p(\mathbf{r})}{|\,\mathbf{r}' - \mathbf{r}\,|}, \;\; A(r) = \frac{G_F}{2^{3/2}}\rho_W(r)$

- In the massless limit(Weyl basis): $\left[\alpha\mathbf{p} + V_{L,R}(r)\right]\Psi_{L,R} = E\psi_{L,R}$, where $V_{L,R}(r) = V(r) \pm A(r)$

Back

Parity violating asymmetry A_{PV}

The observable in PREX and CREX

- Parity violating asymmetry: $A_{PV} = \dfrac{\sigma_R - \sigma_L}{\sigma_R + \sigma_L}$

  where σ_R, σ_L are crossection of the scattering problem:

  $\left[\alpha \mathbf{p} + V_{L,R}(r)\right] \Psi_{L,R} = E\psi_{L,R}$, where $V_{L,R}(r) = V(r) \pm A(r)$,

  $V(r) = \displaystyle\int d^3\mathbf{r}' \frac{\rho_p(\mathbf{r})}{|\mathbf{r}' - \mathbf{r}|}, \quad A(r) = \frac{G_F}{2^{3/2}} \rho_W(r)$

  which is called "Coulomb distortion" in this context:

  Coulomb distortion stands forrepeated electromagnetic interactions with the nucleus remaining in its ground state. This is of order $Z\alpha/\pi$, 20 % for 208Pb.

Form Factor

- Point charge Coulomb (Mott) scattering: $\left[\frac{d\sigma}{d\Omega}\right]_{Mott} = \frac{Z^2 e^4 (1 - \beta^2 \sin^2 \frac{\theta}{2})}{64\pi^2 \varepsilon_0^2 p^2 \beta^2 \sin^2 \frac{\theta}{2}}$
- Extended Coulomb scattering: $-\frac{Ze^2}{r} \longrightarrow e^2 \int \frac{\rho(r') d^3 r'}{|r - r'|}$

$$\frac{d\sigma}{d\Omega} = \left[\frac{d\sigma}{d\Omega}\right]_{Mott} |F(\mathbf{q})|^2$$

$$F(\mathbf{q}) = \frac{1}{Q}\int e^{i\mathbf{q}\cdot\mathbf{r}} \rho(\mathbf{r}) d^3 r = \frac{1}{Q}\int \left(1 + i\mathbf{q}\cdot\mathbf{r} - \frac{1}{2}(\mathbf{q}\cdot\mathbf{r})^2 + \ldots\right) \rho(\mathbf{r}) d^3 r$$

$$= 1 - \frac{1}{6} q^2 < r^2 > + \ldots$$ assuming spherical symmetry

- At small q, $\lim_{q << \sqrt{< r^2 >}} < r^2 > = \frac{6[1 - F(q)]}{q^2}$

Back

Born approximation

- Axial weak potential, $A(r) = \dfrac{G_F}{2^{3/2}}\rho_W(r)$
- Scattering amplitude:
$$\int < \psi_{in}|A(r)|\psi_{out} > d^3r = \frac{G_F}{2^{3/2}}\int e^{i\mathbf{q}\cdot\mathbf{r}}\rho_W(\mathbf{r})d^3r = \frac{G_F Q_W}{2^{3/2}q^2}F_W(q)$$
- $A_{PV} = \dfrac{\sigma_R - \sigma_L}{\sigma_R + \sigma_L} \approx \dfrac{G_F q^2 |Q_W|}{4\sqrt{2}\pi\alpha Z}\dfrac{F_W(q)}{F_E(q)} \propto \dfrac{(F_E + F_W)^2 - (F_E - F_W)^2}{(F_E + F_W)^2 + (F_E - F_W)^2}$

where $F(q) = \dfrac{\int j_0(qr)\rho(r)d^3r}{\int \rho(r)d^3r}$, and $j_0(qr) = \dfrac{\sin(qr)}{qr}$ is spherical Bessel function

Back

Weak Charge of Nuclei

- Weak charge: $Q_W = 2T_3 - 4Q_E \sin^2(\Theta_W)$
  where weak isospin $T_3 = -\frac{1}{2}$ for electron, up quark and neutron, $\frac{1}{2}$ for neutrino, down quark and proton
- Neutron weak charge: $Q_n = -1$ (–0.9878 with radiative correction)
  Proton weak charge $Q_p = 1 - 4\sin^2(\Theta_W)$ (0.0721 with radiative correction)
- Neutron form factor: $G_n^W = Q_n G_p^E + Q_p G_n^E + Q_n G_s^E$
  Proton form factor: $G_p^W = Q_p G_p^E + Q_n G_n^E + Q_n G_s^E$
- Weak charge distribution: $\rho_W(r) = \int d^3r' \left[G_n^W(r - r')\rho_n(r) + G_p^W(r - r')\rho_p(r) \right]$
- Electric charge distribution: $\rho_E(r) = \int d^3r' \left[G_n^E(r - r')\rho_n(r) + G_p^E(r - r')\rho_p(r) \right]$
- Additional complicity: many-body correction, center-of-mass correction, the magnetic contribution from spin-orbital current(SHF) or tensor density (RMF)

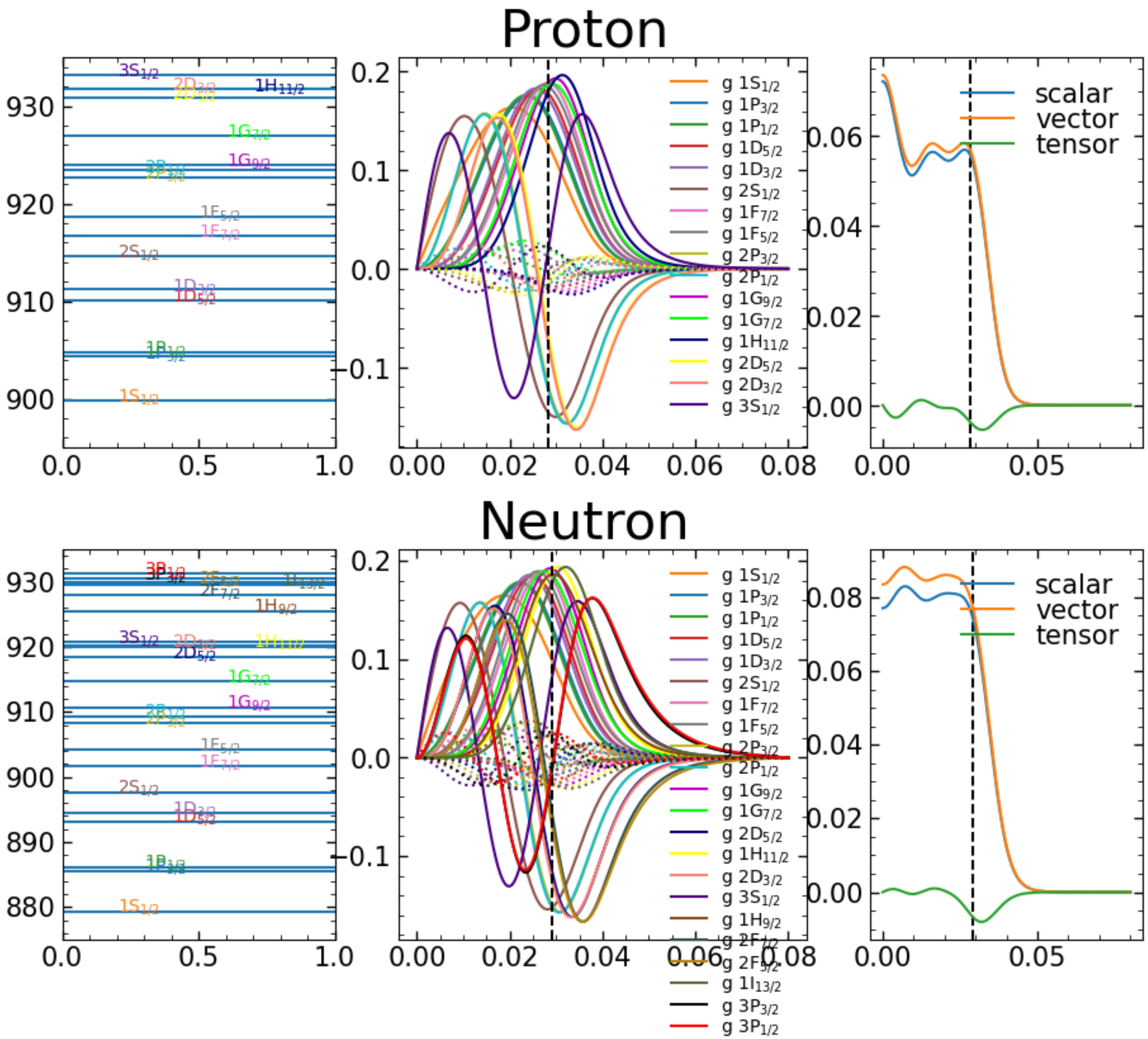
Proton
Neutron
scalar
vector
tensor
g 1S1/2
g 1P3/2
g 1P1/2
g 1D5/2
g 1D3/2
g 2S1/2
g 1F7/2
g 1F5/2
g 2P3/2
g 2P1/2
g 1G9/2
g 1G7/2
g 1H11/2
g 2D5/2
g 2D3/2
g 3S1/2
g 1H9/2
g 2F7/2
g 2F5/2
g 1I13/2
g 3P3/2
g 3P1/2

		Experiment	NL3	FSU2	IOPB-I	IUFSU	BigApple	HPUC	BSRV	DINOa	DINOb	DINOc	CPREX1	CPREX2
^{208}**Pb**	B/A [MeV]	7.87	7.88	7.87	7.86	7.88	7.85	7.85	7.84	7.87	7.87	7.87	7.84	7.86
	R_{ch} [fm]	5.50	5.51	5.49	5.52	5.49	5.50	5.56	5.53	5.51	5.51	5.51	5.49	5.49
	ΔR_{np} [fm]	0.159$\pm$ 0.017	0.2797	0.2862	0.2195	0.1618	0.1508	0.1196	0.2595	0.1746	0.1993	0.2235	0.1905	0.1525
	F_{ch} []	0.409	0.4067	0.4094	0.4052	0.4106	0.4080	0.3992	0.4043	0.4074	0.4075	0.4073	0.4100	0.4092
	ΔF []	0.041$\pm$0.013	0.0414	0.0423	0.0319	0.0233	0.0214	0.0168	0.0378	0.0262	0.0303	0.0342	0.0282	0.0222
^{48}**Ca**	B/A [MeV]	8.67	8.65	8.62	8.64	8.53	8.52	8.65	8.66	8.67	8.67	8.67	8.64	8.66
	R_{ch} [fm]	3.48	3.45	3.43	3.45	3.44	3.46	3.46	3.44	3.47	3.47	3.47	3.48	3.46
	ΔR_{np} [fm]	0.137$\pm$0.015	0.2255	0.2318	0.1995	0.1736	0.1690	0.1479	0.2196	0.0994	0.1054	0.1141	0.1252	0.1357
	F_{ch} []	0.158	0.1604	0.1665	0.1616	0.1647	0.1582	0.1577	0.1621	0.1591	0.1589	0.1585	0.1537	0.1571
	ΔF []	0.0277$\pm$0.0055	0.0551	0.0564	0.0490	0.0435	0.0413	0.0391	0.0527	0.0330	0.0345	0.0364	0.0335	0.0362

TABLE I. Experimental data for the binding energy per nucleon[1], charge radii[2], neutron skins (excluding PREX and CREX)[3], charge from factor and form factor difference from PREX[4] for ^{208}Pb and CREX[5] for ^{48}Ca. Also displayed are the theoretical results obtained with NL3[6], FSUGold2[7], IOPB-I[8], IUFSU[9], BigApple[10], HPUC[11], BSRV[12], DINOa-c[13] and the two new parameterizations, CPREX1 and CPREX2.

		NL3	FSU2	IOPB-I	IUFSU	BigApple	HPUC	BSRV	DINOa	DINOb	DINOc	CPREX1	CPREX2
SNM	n_s [fm^{-3}]	0.1483	0.1504	0.1495	0.1546	0.1546	0.1490	0.1480	0.1522	0.1525	0.1519	0.1516	0.1518
	M^* [MeV]	558.7	557.0	557.2	572.1	572.8	572.9	565.3	587.4	593.0	593.9	692.8	648.1
	B [MeV]	16.24	16.26	16.10	16.40	16.34	15.98	16.10	16.16	16.21	16.21	16.29	16.14
	K [MeV]	271.6	237.7	222.6	231.3	227.0	220.2	227.2	210.0	207.0	206.0	223.8	223.5
	S_V [MeV]	37.3	37.6	33.3	31.3	31.3	28.4	36.1	31.4	33.1	34.6	32.9	29.8
	L [MeV]	118.2	112.7	63.6	47.2	39.8	41.6	84.6	50.0	70.0	90.0	-3.5	0.4
	K_{sym} [MeV]	101.0	25.4	-37.0	28.5	87.5	81.1	-73.2	506.0	609.1	714.8	-418.4	-239.8
PNM	M^*_n [MeV]	569.2	566.0	566.7	580.5	582.8	581.4	573.3	352.1	333.0	320.5	377.4	465.6
	M^*_p [MeV]	569.2	566.0	566.7	580.5	582.8	581.4	574.8	908.8	948.2	969.1	1062.5	870.1
	S_V [MeV]	38.3	38.6	34.7	32.9	33.1	29.9	37.2	46.5	50.6	53.4	54.3	38.4
	L [MeV]	121.2	115.9	67.7	49.5	40.6	42.7	88.7	172.1	216.4	247.8	211.2	75.9
	K_{sym} [MeV]	100.3	27.2	-45.5	23.1	74.3	89.2	-70.6	726.7	907.2	1021.2	801.8	76.4
NS	M_{max} [$M_\odot$]	2.77	2.07	2.15	1.94	2.60	2.05	2.04	2.17	2.15	2.15	2.04	2.12
	$R_{1.0}$ [km]	14.4	14.1	13.2	12.6	12.8	12.6	13.6	14.4	14.8	15.1	13.9	12.9
	$R_{1.4}$ [km]	14.5	13.9	13.2	12.6	13.1	12.8	13.4	14.4	14.6	14.9	13.4	12.9
	$\Lambda_{1.0}$ []	7797	6473	4347	3384	3918	3752	4903	6623	7572	8579	4543	3544
	$\Lambda_{1.4}$ []	1275	876	687	500	719	593	689	1065	1150	1256	584	570

TABLE II. Saturation properties and neutron star properties of RMF models listed in Table I. Saturation properties for SNM and PNM are defined in the letter. Neutron star properties are calculated with the crust EOSs constructed with the compressible liquid droplet model repectively for various RMF models with fixed surface tension parameters $\sigma_s = 1.2$ MeV fm^{-2}, $S_S = 48$ MeV[14].

Neutron star EOS

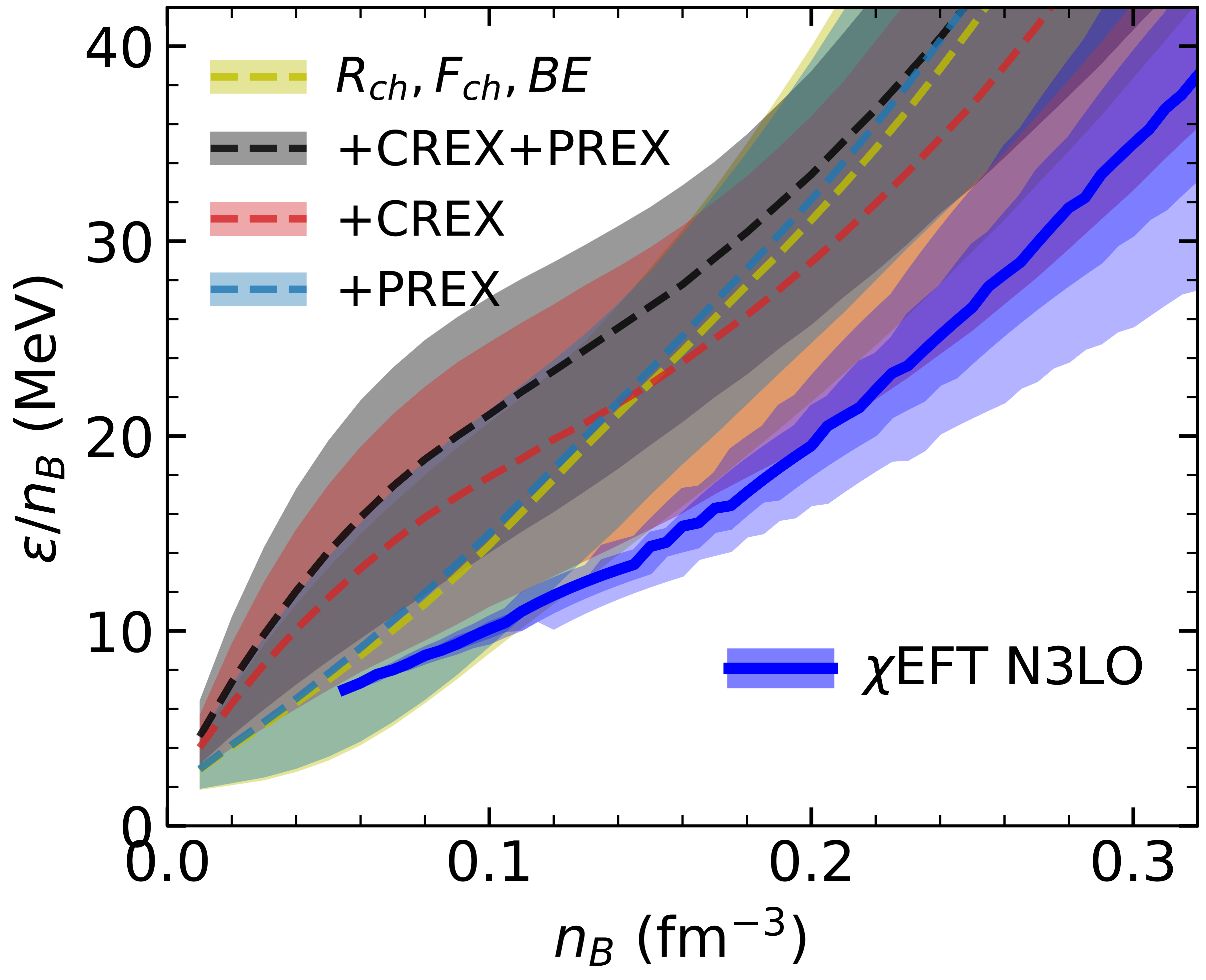

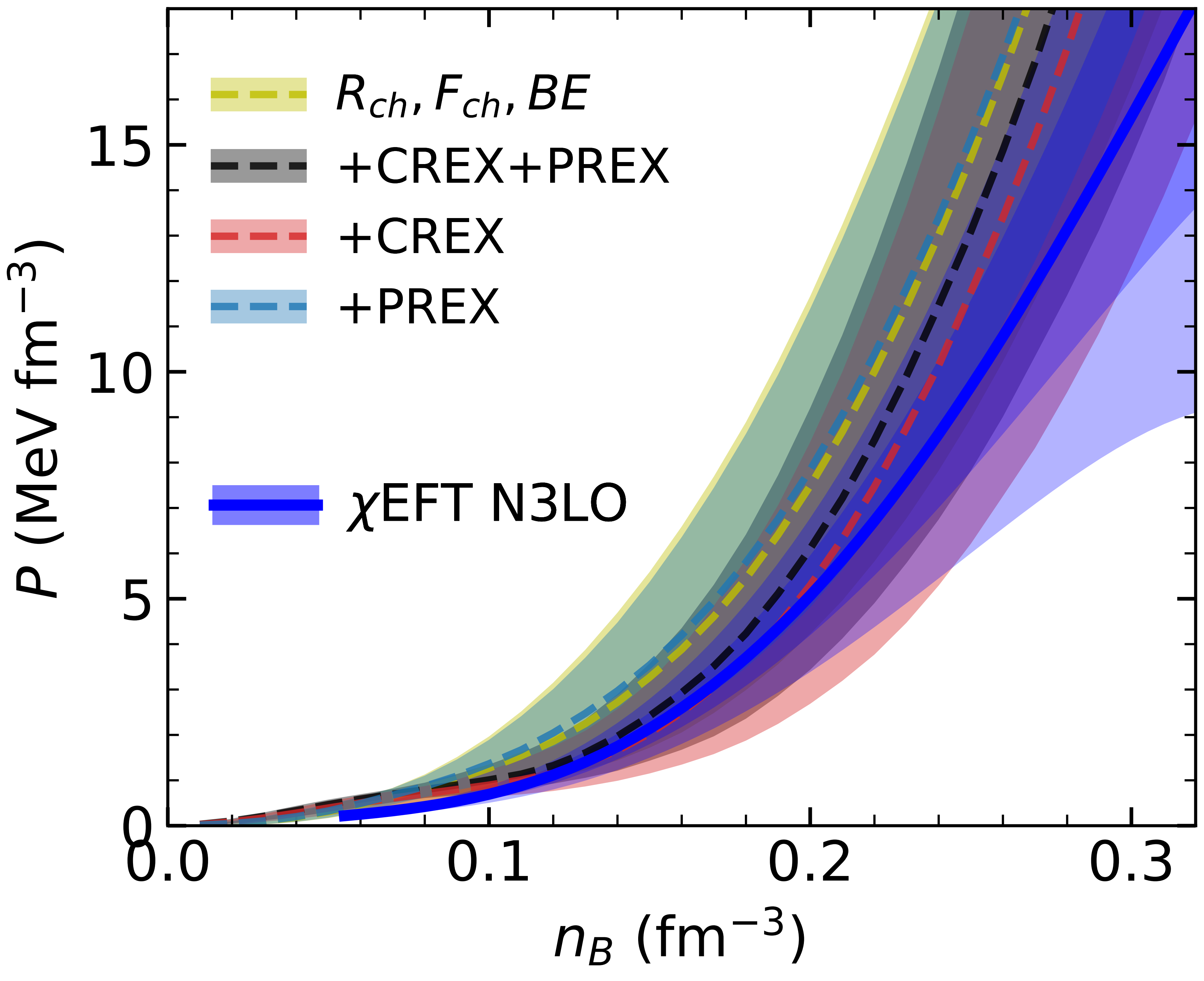

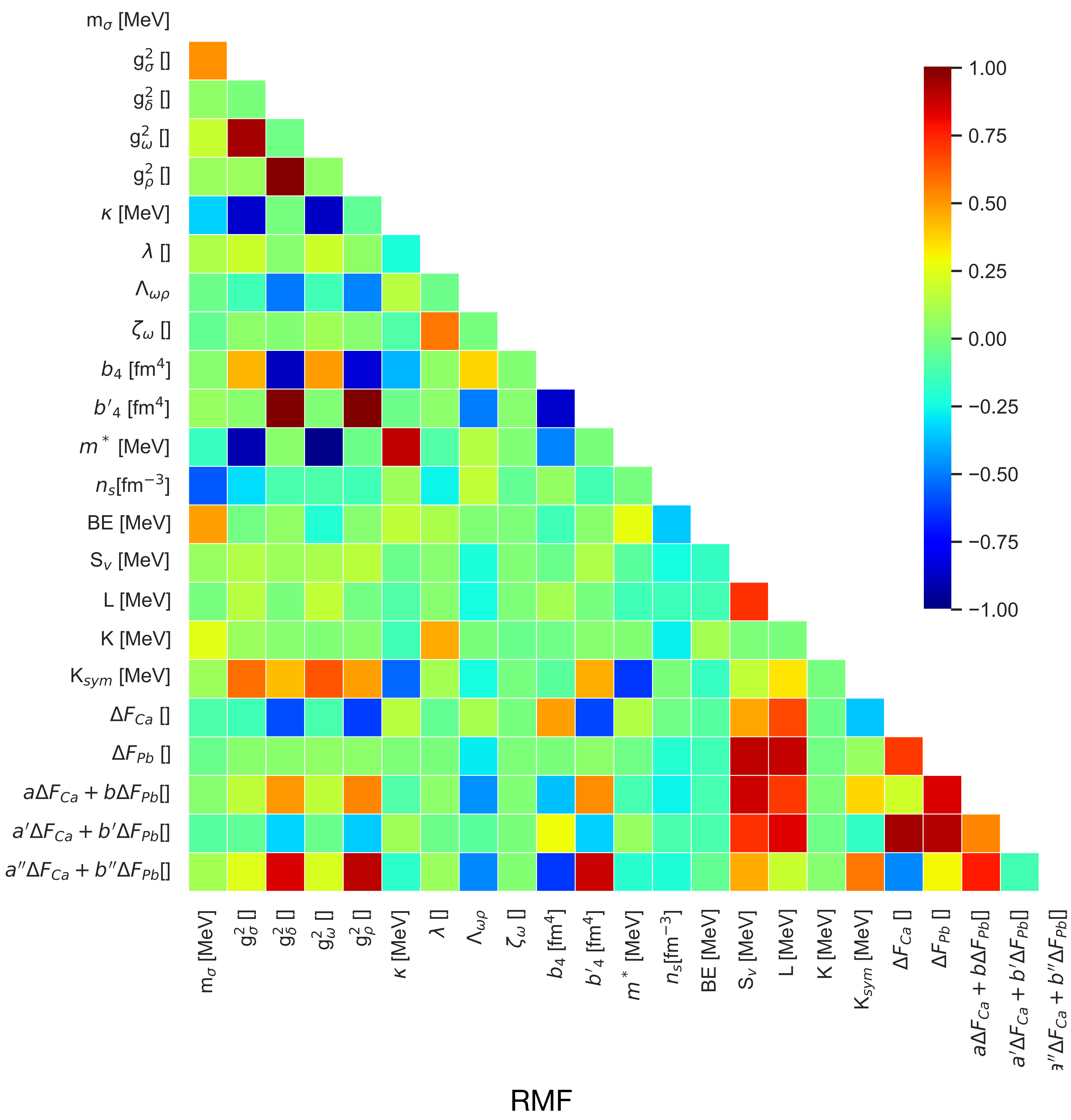
m$_\sigma$ [MeV]
g$^2_\sigma$ []
g$^2_\delta$ []
g$^2_\omega$ []
g$^2_\rho$ []
κ [MeV]
λ []
$\Lambda_{\omega\rho}$
ζ_ω []
b_4 [fm^4]
b'_4 [fm^4]
m^* [MeV]
n_s[fm^{-3}]
BE [MeV]
S$_v$ [MeV]
L [MeV]
K [MeV]
K$_{sym}$ [MeV]
ΔF_{Ca} []
ΔF_{Pb} []
$a\Delta F_{Ca} + b\Delta F_{Pb}$[]
$a'\Delta F_{Ca} + b'\Delta F_{Pb}$[]
$a''\Delta F_{Ca} + b''\Delta F_{Pb}$[]
1.00
0.75
0.50
0.25
0.00
−0.25
−0.50
−0.75
−1.00
RMF

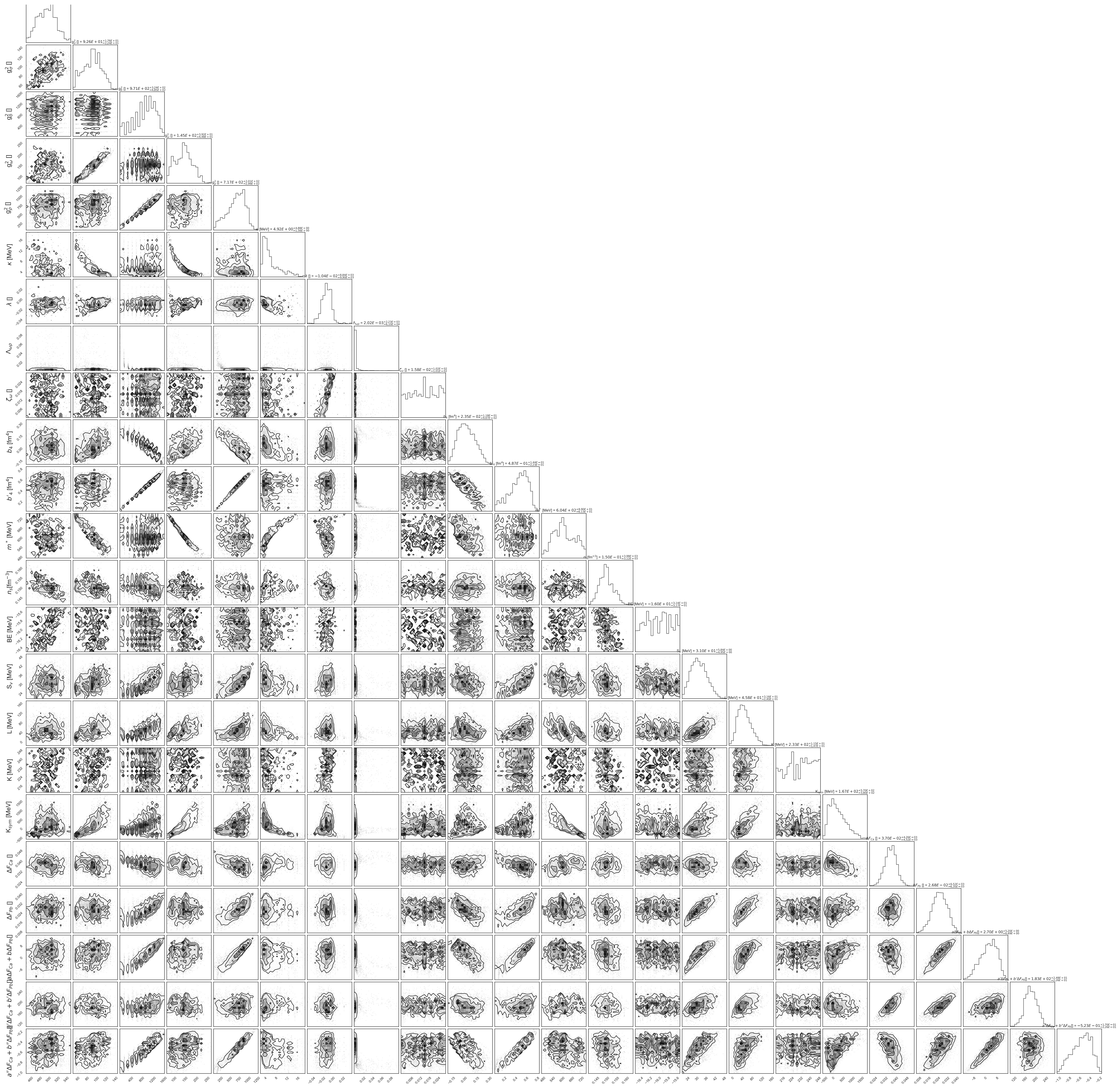

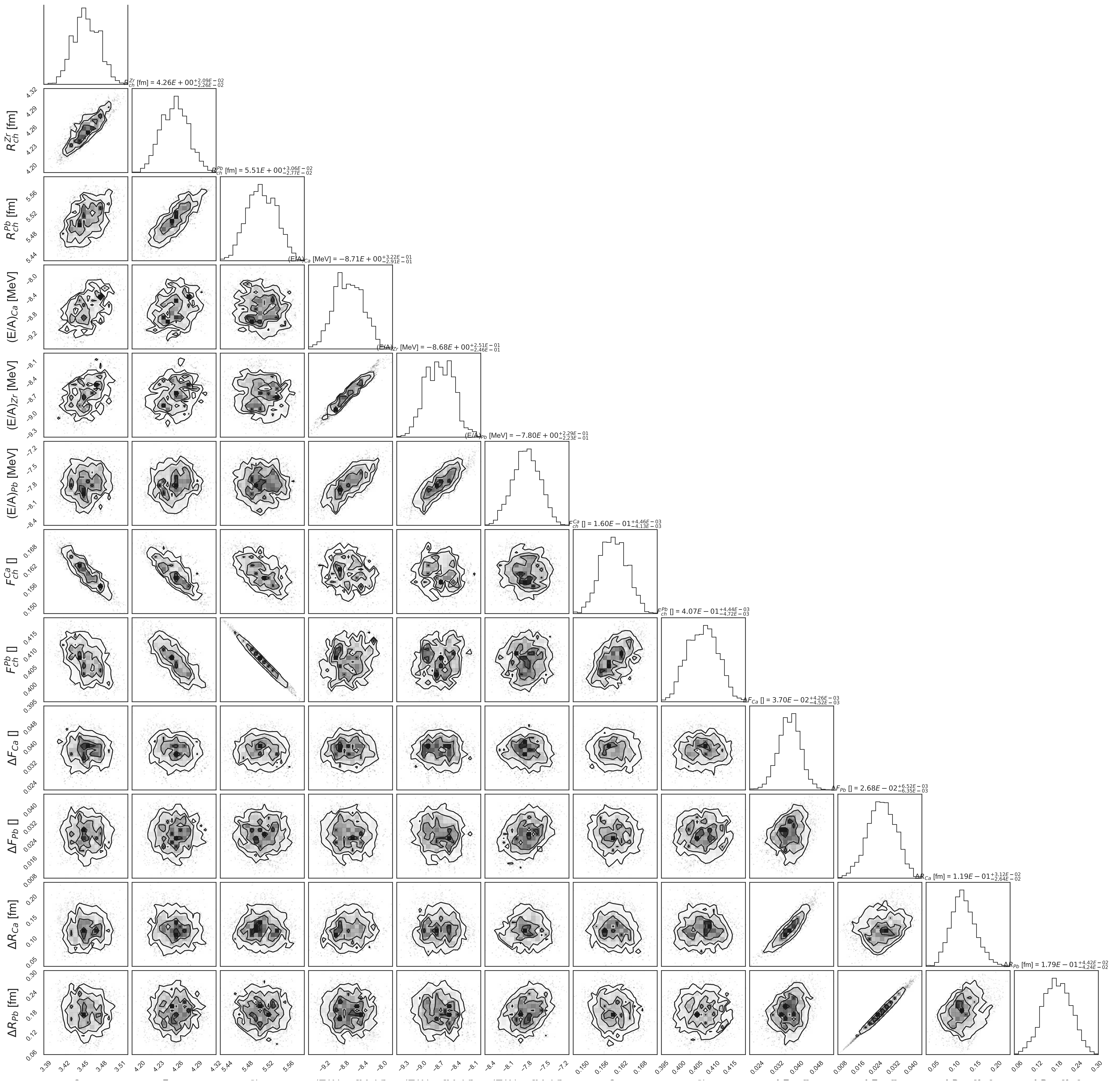

R^{Zr}_{ch} [fm] = $4.26E+00^{+2.09E-02}_{-2.26E-02}$
R^{Pb}_{ch} [fm] = $5.51E+00^{+3.06E-02}_{-2.77E-02}$
$(E/A)_{Ca}$ [MeV] = $-8.71E+00^{+3.22E-01}_{-2.91E-01}$
$(E/A)_{Zr}$ [MeV] = $-8.68E+00^{+2.51E-01}_{-2.46E-01}$
$(E/A)_{Pb}$ [MeV] = $-7.80E+00^{+2.29E-01}_{-2.23E-01}$
F^{Ca}_{ch} [] = $1.60E-01^{+4.46E-03}_{-4.13E-03}$
F^{Pb}_{ch} [] = $4.07E-01^{+4.44E-03}_{-4.72E-03}$
ΔF_{Ca} [] = $3.70E-02^{+4.26E-03}_{-4.52E-03}$
ΔF_{Pb} [] = $2.68E-02^{+6.57E-03}_{-6.35E-03}$
ΔR_{Ca} [fm] = $1.19E-01^{+3.12E-02}_{-2.64E-02}$
ΔR_{Pb} [fm] = $1.79E-01^{+4.42E-02}_{-4.24E-02}$
R^{Zr}_{ch} [fm]
R^{Pb}_{ch} [fm]
$(E/A)_{Ca}$ [MeV]
$(E/A)_{Zr}$ [MeV]
$(E/A)_{Pb}$ [MeV]
F^{Ca}_{ch} []
F^{Pb}_{ch} []
ΔF_{Ca} []
ΔF_{Pb} []
ΔR_{Ca} [fm]
ΔR_{Pb} [fm]

RMF